Instability and Phase Transition in Asymmetric Nuclei

Kyung Hee University
Suk-Joon Lee

HIM-2009-9-26

Thermalized nuclear system

Medium energy heavy-ion collision

RIB - Asymmetric

Neutron star

Short range repulsive and long range attractive

Saturation, Phase transition

Tow component system: 3-d of $\rho = \rho_p + \rho_n, y = \rho_p / \rho$, T

^{3}He, Binary alloy

Phase diagram; surface in 3-d of P, T, y or density

Symmetry energy

Second order transition, Isospin fractionation

Coulomb energy

Beta stability line $Z \neq N$, Asymmetric phase diagram

Finite system

Surface energy

Velocity dependent interaction

Effective mass

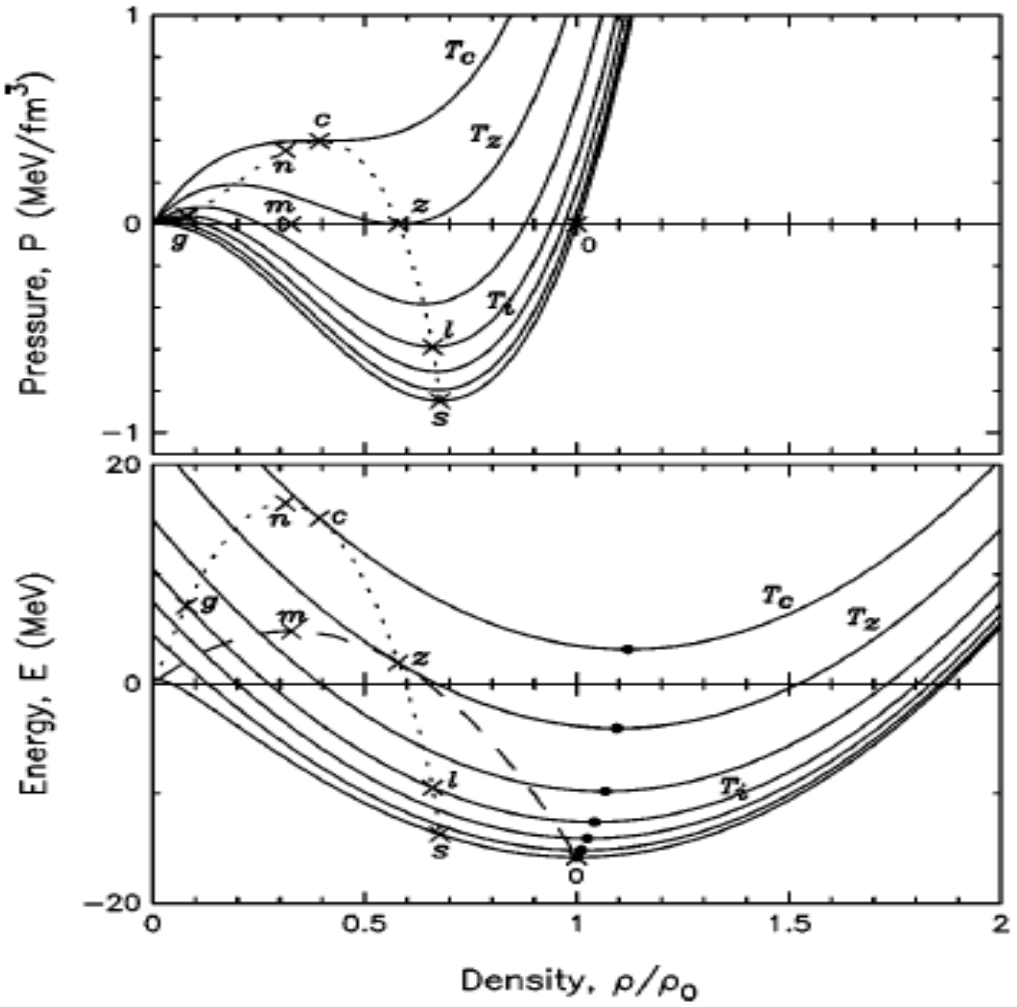

FIG. 1. Equation of state of nuclear matter [5] for temperature T of, from bottom to top, 0, 3, 5, 7, 10, 15.16 (T_z at which the minimum pressure is zero), and 20.95 (which is the critical temperature T_c) in MeV. Also shown are the spinodal points (dotted line), the points with zero pressure (dashed line), and the points of minimum energy (solid circles) for each temperature T. See the text for variously marked points of cross.

S.J. Lee
A.Z. Mekjian
PRC56,2621(1997)

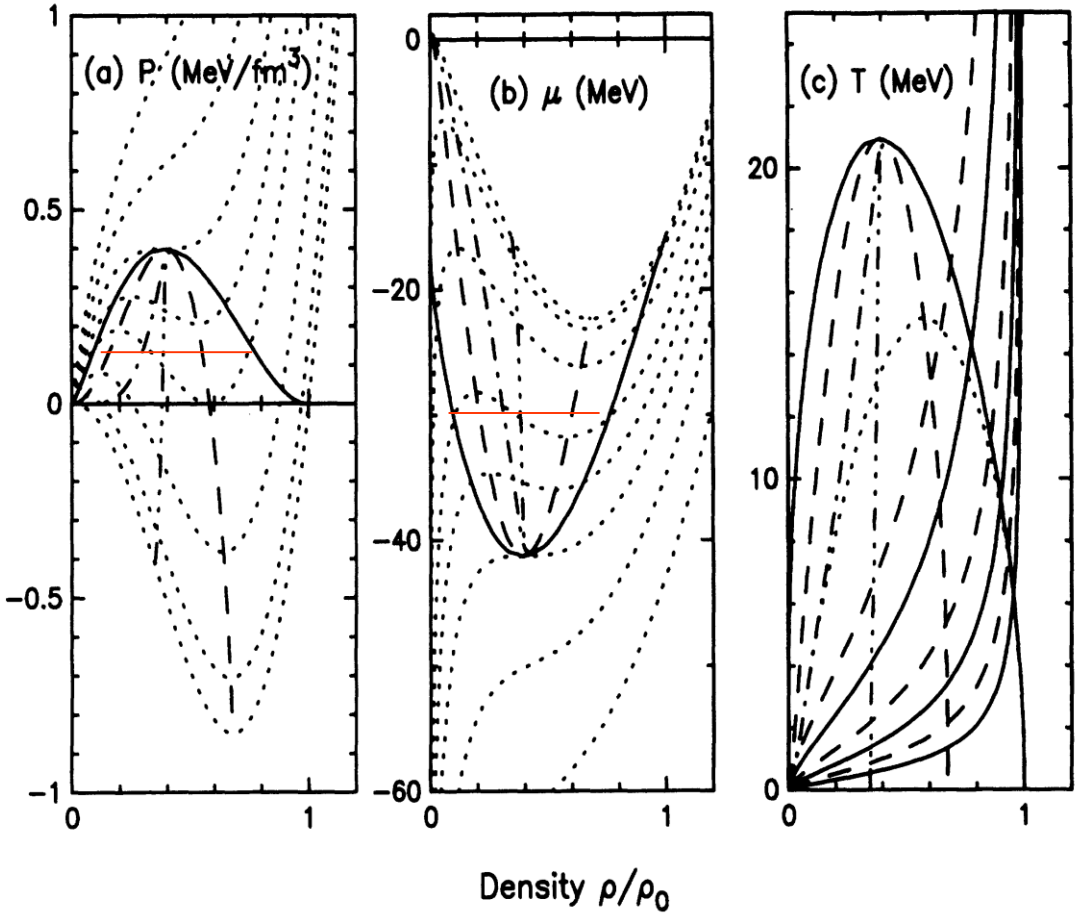

S.J.Lee
A,Z,Mekjian
PRC45,1284(192)

FIG. 4. (a) Equation of state ($P-\rho$) for nuclear matter with BKN force parameters [17] at various temperatures (dotted line). Each dotted line represents the density dependence of the pressure at a temperature T of 0 MeV, 5 MeV, 10 MeV, 15.16 MeV (at which the minimum pressure is 0), 18 MeV, 20.95 MeV [which is the critical temperature T_c (read from bottom up)] 25 MeV, and 30 MeV. (b) The density dependence of the chemical potential μ at various temperatures (dotted line). The temperatures are the same as in (a) but starting from the top. In both (a) and (b), the solid curve is for the coexistent line and the dashed curve is for the spinodal line. The dash-dotted (dash-dot-dot-dotted) line indicate the densities with the same pressure P (chemical potential μ) as the coexistent line at each temperature. (c) The density dependence of the temperatures on the lines mentioned above. The dotted line in (c) is for the density with zero pressure for a given temperature. Here the densities for $X_0(T)=1$ [$X_0(T)=2$] of Eq. (87) with Eq. (96) are also shown as solid (dashed) lines for, from top to bottom, $A=10$, 50, and 200.

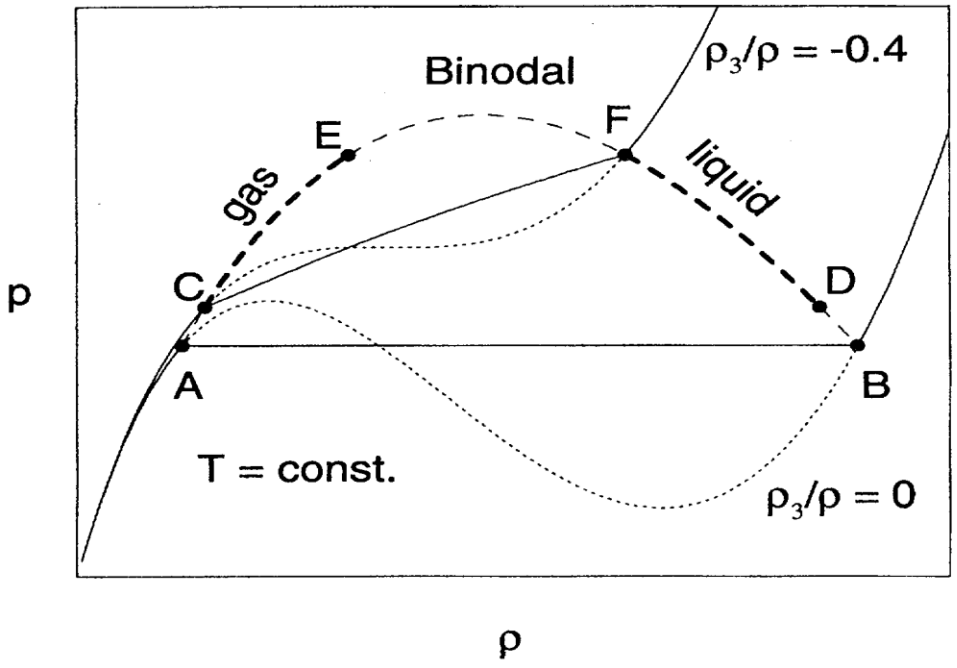

FIG. 3. The Maxwell construction for symmetric and asymmetric systems. The construction for symmetric matter ($\rho_3/\rho = 0$) is indicated by the segment AB and is the same as for a one-component system. The construction for asymmetric matter with $\rho_3/\rho = -0.4$ is indicated by the segment CF and shows the qualitatively new behavior allowed in a two-component system. The asymmetry is held constant throughout the phase separation. The (dashed) binodal line is obtained from similar isotherms at other values of the asymmetry.

H. Mueller and B,D. Serot, PRC.52, 2072 (1995)

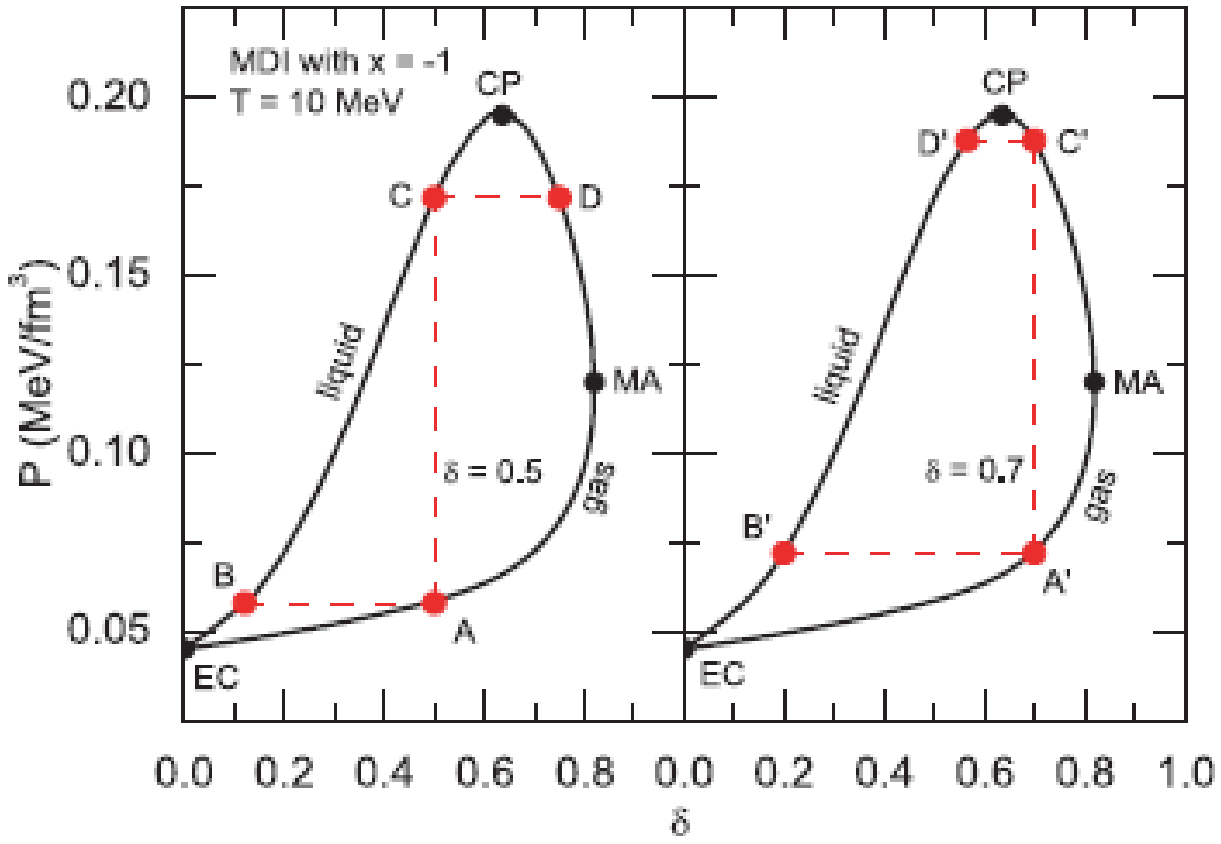

J. Xu, L.W. Chen, B.A, Li, and H.L. Ma
PRC77, 014302(2008)

FIG. 24. (Color online) The binodal surface at 10 MeV in the MDI interactions with $x = -1$ is plotted to show the phase-transition process. The points A (A′) through C (C′) denote phases participating in a phase transition.

$$f_q(\vec{r},\vec{p}) = \frac{\gamma}{h^2}\,\tilde{f}_q(\vec{r}_q,\vec{p}) = \frac{\gamma}{h^2}\;\frac{1}{1+e^{\beta[\varepsilon_q(\vec{r},\vec{p})-\mu_q]}} = \frac{\gamma}{h^2}\;\frac{1}{1+e^{\beta\frac{p^2}{2m_q^*}-\eta_q}}$$

$$\rho_q = \sum_{i\in q}\left|\psi_i(\vec{r})\right|^2 = \int d^3p \quad f_q(\vec{r},\vec{p})$$

$$\tau_q = \sum_{i\in q}\left|\vec{\nabla}\psi_i(\vec{r})\right|^2 = \int d^3p \;\; \frac{p^2}{\hbar^2} \quad f_q(\vec{r},\vec{p})$$

$$\vec{j}_q = \mathrm{Im}\sum_{i\in q}\psi_i^+(\vec{r})\vec{\nabla}\psi_i(\vec{r}) = \int d^3p \;\; \frac{\vec{p}}{\hbar} \quad f_q(\vec{r},\vec{p})$$

$$\vec{J}_q = \sum_{i\in q}\psi_i^+(\vec{r})\vec{\sigma}\times\vec{\nabla}\psi_i(\vec{r}) = \int d^3p \;\; \frac{i\vec{\sigma}\times\vec{p}}{\hbar} \quad f_q(\vec{r},\vec{p})$$

$$H = H_B + H_S + H_C + H_J \qquad\qquad H_B = H_K + U_B$$

$$h_q(\vec{r},\vec{p}) = \frac{\delta H}{\delta f(\vec{r},\vec{p})} \qquad\qquad h_q(\vec{r},\vec{p})\psi_q(\vec{r}) = \varepsilon_q(\vec{p})\psi_q(\vec{r})$$

Thermodynamic Variables

Momentum conservation: $\frac{d}{dt}\left[\int d^3r \int d^3p\, \vec{p} f\right] = -\int d^3r\, \vec{\nabla}\cdot\overleftrightarrow{\Pi} = 0$

$$P = \Pi_{ii} = \sum_q \int d^3p\, p p_i \left(\nabla_p^i \varepsilon_q\right) f_q + \delta_{ii}\left[\sum_q \int d^3p\, \varepsilon_q f_q - E\right]$$

$$= \sum_q \frac{2}{3} E_{Kq}^* + \sum_q \left[\left(\frac{\partial E}{\partial \tau_q}\right)\tau_q + \left(\frac{\partial E}{\partial \rho_q}\right)\rho_q - \vec{\nabla}\cdot\left(\frac{\partial E}{\partial \vec{\nabla}\rho_q}\right)\rho_q\right] - E$$

$$S_q = -\frac{\gamma}{h^3}\int d^3p\left[\tilde{f}_q \ln \tilde{f}_q + \left(1-\tilde{f}_q\right)\ln\left(1-\tilde{f}_q\right)\right]$$

$$= \beta\int d^3p\, \varepsilon_q f_q + \beta\int d^3p\, \frac{\vec{p}\cdot\vec{\nabla}_p \varepsilon_q}{3} f_q - \beta\mu_q \int d^3p\, f_q$$

$$TS = E + P - \sum_q \mu_q \rho_q$$

Coexistence ; Gibbs conditions

$$P^i = P^j$$
$$\mu_q^i = \mu_q^j$$

at same T but not necessarily $\rho_q^i = \rho_q^j$

Critical point

$$\frac{\partial P}{\partial \rho_q} = \frac{\partial^2 P}{\partial \rho_q^2} = 0 \qquad \frac{\partial \mu_q}{\partial \rho_q} = \frac{\partial^2 \mu_q}{\partial \rho_q^2} = 0$$

$$\rho = \rho_p + \rho_n$$
$$y = \rho_p / \rho$$

Spinodal

For mechanical instability: $\left.\frac{\partial P}{\partial \rho}\right|_{y,T} = 0$

$$E - TS - \mu_p \rho_p - \mu_n \rho_n = -P$$
$$\rho_p d\mu_p + \rho_n d\mu_n = dP$$

For chemical instability: $\left.\frac{\partial \mu_q}{\partial y}\right|_{P,T} = 0$

Equal concentration or extremum of $y(\rho)|_{P,T}$

$$\frac{\partial P}{\partial y} = 0 \quad \text{and} \quad \frac{\partial \rho}{\partial y} = 0 \quad \text{at} \quad y = y_m(\rho)$$

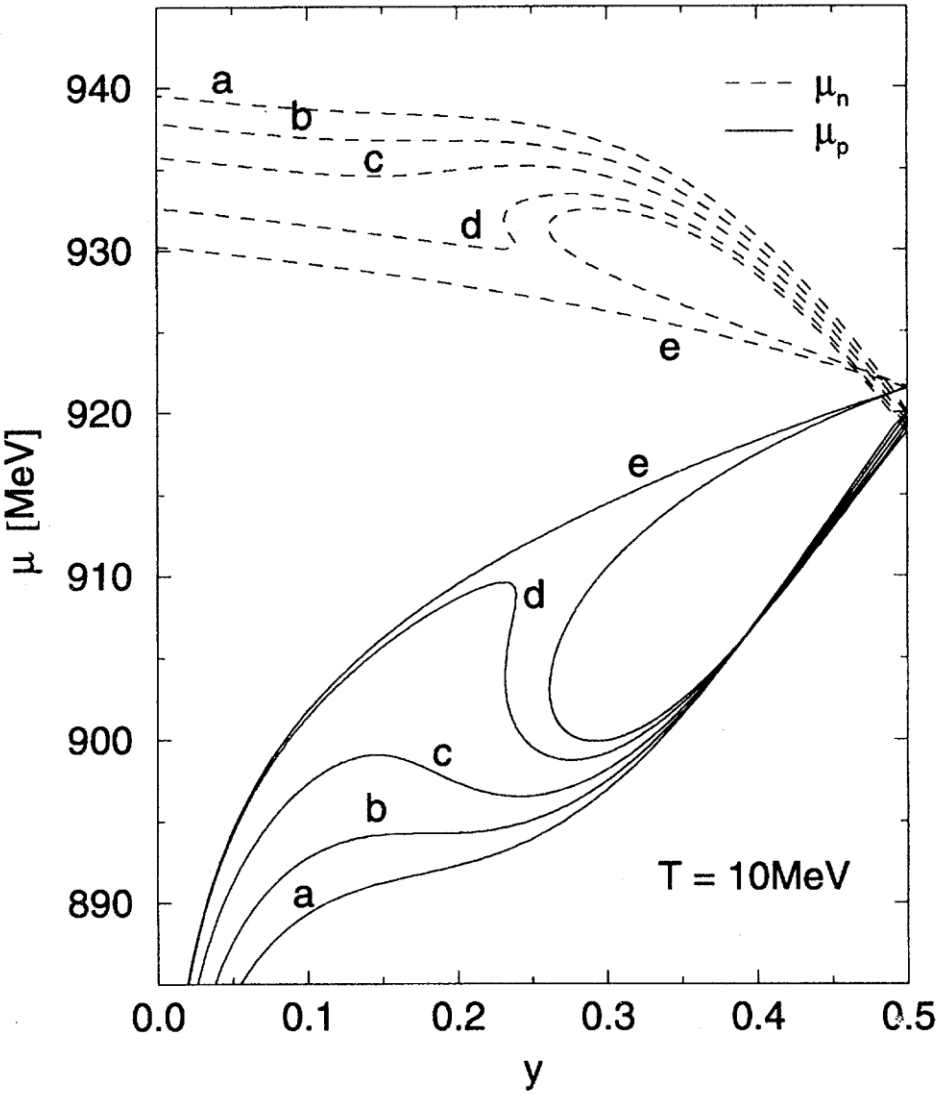

$\mu_q(y,P,T)$

FIG. 5. Chemical potential isobars at fixed temperature as a function of y. The curves labeled a through e have pressures $p=0.25,0.198,0.15,0.10,0.075$ MeV/fm^3, respectively. The curves labeled b are at the critical pressure $p_c=0.198$ MeV/fm^3.

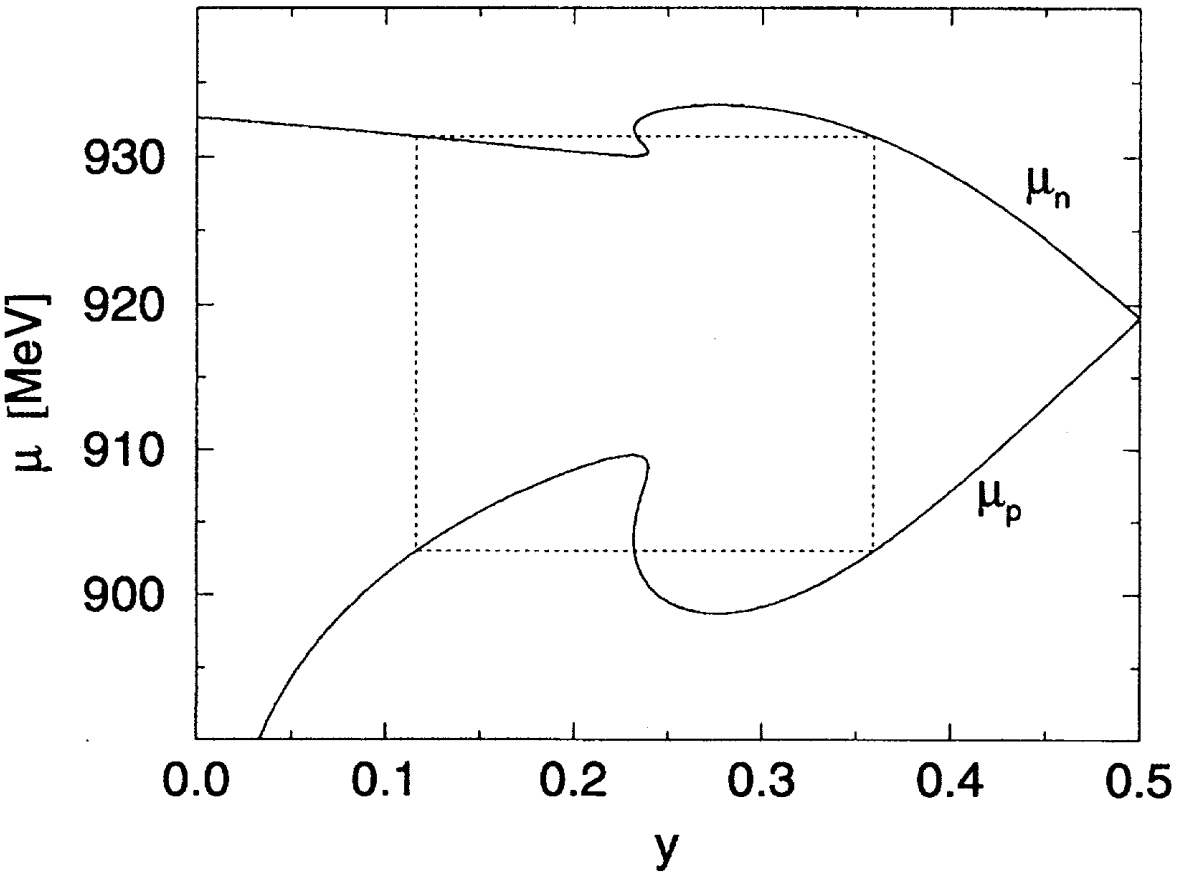

FIG. 6. Geometrical construction used to obtain the proton fractions and chemical potentials in the two coexisting phases at fixed $T = 10$ MeV and $p = 0.1$ MeV/fm^3.

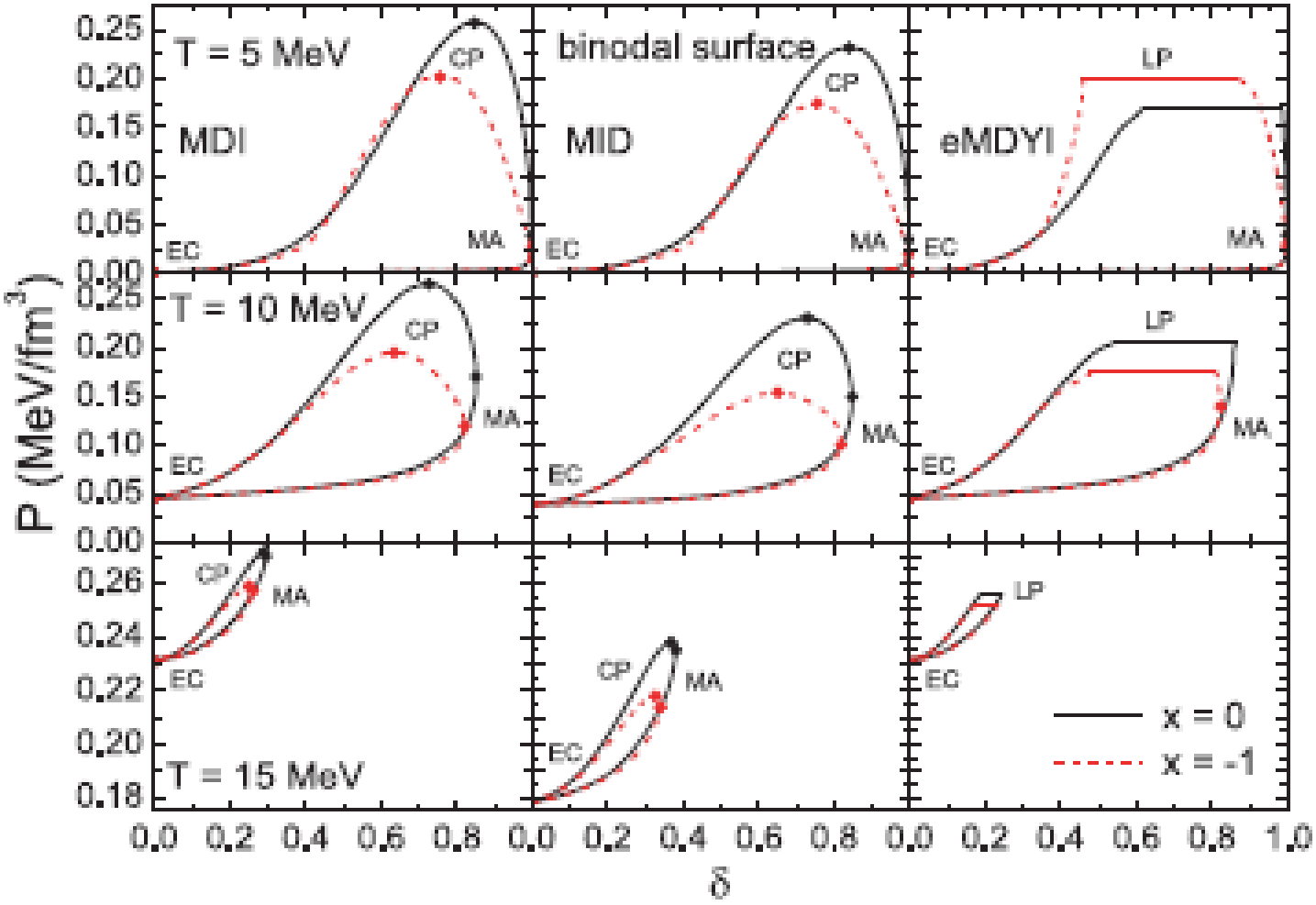

FIG. 23. (Color online) The section of binodal surface at $T = 5$, 10, and 15 MeV in the MDI, MID, and eMDYI interactions with $x = 0$ and $x = -1$. The critical pressure (CP), the limiting pressure (LP), the points of equal concentration (EC), and maximal asymmetry (MA) are also indicated.

Skyrme Hamiltonian

$$H = \frac{\hbar^2}{2m_p}\tau_p + \frac{\hbar^2}{2m_n}\tau_n$$

$$+ \frac{1}{4}\left[t_1\left(1+\frac{x_1}{2}\right) + t_2\left(1+\frac{x_2}{2}\right)\right]\rho\tau - \frac{1}{4}\left[t_1\left(\frac{1}{2}+x_1\right) - t_2\left(\frac{1}{2}+x_2\right)\right]\left(\rho_p\tau_p + \rho_n\tau_n\right)$$

$$+ \frac{t_0}{2}\left[\left(1+\frac{x_0}{2}\right)\rho^2 - \left(\frac{1}{2}+x_0\right)\left(\rho_p^2+\rho_n^2\right)\right]$$

$$+ \frac{t_3}{12}\left[\left(1+\frac{x_3}{2}\right)\rho^2 - \left(\frac{1}{2}+x_3\right)\left(\rho_p^2+\rho_n^2\right)\right]\rho^\alpha + H_C + H_S + H_j$$

$$H_S = \frac{1}{16}\left[3t_1\left(1+\frac{x_1}{2}\right) - t_2\left(1+\frac{x_2}{2}\right)\right]\left(\vec{\nabla}\rho\right)^2$$

$$- \frac{1}{16}\left[3t_1\left(\frac{1}{2}+x_1\right) + t_2\left(\frac{1}{2}+x_2\right)\right]\left[\left(\vec{\nabla}\rho_p\right)^2 + \left(\vec{\nabla}\rho_n\right)^2\right] \approx C_S\rho^\eta$$

$$H_j = -\frac{1}{4}\left[t_1\left(1+\frac{x_1}{2}\right) + t_2\left(1+\frac{x_2}{2}\right)\right]j^2 + \frac{1}{4}\left[t_1\left(\frac{1}{2}+x_1\right) - t_2\left(\frac{1}{2}+x_2\right)\right]\left(j_p^2 + j_n^2\right)$$

$$H_C \approx C\rho^\beta\rho_p^2 \qquad C\rho^\beta = \frac{4\pi}{3}e^2R^2 \qquad C_S\rho^\eta = \frac{4\pi r_0\sigma}{V^{1/3}}\rho^{2/3}$$

Single particle energy

$$h_q(\vec{r},\vec{p}) = \left(\frac{\partial H}{\partial \tau_q}\right)\frac{p^2}{\hbar^2} + \left(\frac{\partial H}{\partial \rho_q}\right) - \vec{\nabla}\cdot\left(\frac{\partial H}{\partial \vec{\nabla}\rho_q}\right)$$

$$\varepsilon_q(\vec{p})\psi_q(\vec{r}) = h_q(\vec{r},\vec{p})\psi_q(\vec{r})$$

$$\mu_q = \int d^3r\,\psi_q^*(\vec{r})h_q(\vec{r},\vec{p})\psi_q(\vec{r}) = \varepsilon_q(p_{Fq})$$

$$= T\eta_q(\rho_q,T) + \left(\frac{\partial E}{\partial \rho_q}\right) - \vec{\nabla}\cdot\left(\frac{\partial E}{\partial \vec{\nabla}\rho_q}\right)$$

$$T\eta_q(\rho_q,T) = \left(\frac{\partial E}{\partial \tau_q}\right)\frac{p_{Fq}^2}{\hbar^2} = \mu_q - \varepsilon_q(\vec{p}) + \left(\frac{\partial E}{\partial \tau_q}\right)\frac{p^2}{\hbar^2}$$

Helmholtz Free Energy

$$F = E - TS$$

$$TS(\rho_q, T) = \frac{5}{3}\sum_q E^*_{Kq}(\rho_q, T) - T\sum_q \eta_q(\rho_q, T)\rho_q$$

$$P = \sum_q \frac{2}{3}E^*_{Kq} + \sum_q \left[\left(\frac{\partial E}{\partial \tau_q} \right)\tau_q + \left(\frac{\partial E}{\partial \rho_q} \right)\rho_q - \vec{\nabla}\cdot\left(\frac{\partial E}{\partial \vec{\nabla}\rho_q} \right)\rho_q \right] - E$$

$$\delta\left[\int d^3r\left(E - TS - \mu_p\rho_p - \mu_n\rho_n\right)\right] = 0$$

$$\mu_q = \left(\frac{\delta E}{\delta \rho_q} \right) - \vec{\nabla}\cdot\left(\frac{\partial E}{\partial \vec{\nabla}\rho_q} \right) - T\left(\frac{\delta S}{\delta \rho_q} \right)$$

$$\frac{\delta}{\delta \rho_q} = \frac{\partial}{\partial \rho_q} + \sum_{q'}\left(\frac{\delta \tau_{q'}}{\delta \rho_q} \right)\left(\frac{\partial}{\partial \tau_{q'}} \right)$$

At low T or high density (nearly degenerated Fermi gas)

$$T\eta_q = \frac{p_{Fq}^2}{2m_q^*} = \frac{\hbar^2}{2m_q^*}\left(\frac{6\pi^2}{\gamma}\right)^{2/3}\left[\rho_q^{2/3} - \frac{\pi^2 m_q^{*2}}{3\hbar^4}\left(\frac{\gamma}{6\pi^2}\right)^{4/3} T^2\rho_q^{-2/3} + \cdots\right]$$

$$\tau_q = \frac{2m}{\hbar^2}E_{Kq} = \frac{2m_q^*}{\hbar^2}E_{Kq}^* = \frac{3}{5}\left(\frac{6\pi^2}{\gamma}\right)^{2/3}\left[\rho_q^{5/3} + \frac{5\pi^2 m_q^{*2}}{3\hbar^4}\left(\frac{\gamma}{6\pi^2}\right)^{4/3} T^2\rho_q^{1/3} + \cdots\right]$$

$$TS = \sum_q \frac{\hbar^2}{2m_q^*}\left(\frac{6\pi^2}{\gamma}\right)^{2/3}\left[\frac{2\pi^2 m_q^{*2}}{\hbar^4}\left(\frac{\gamma}{6\pi^2}\right)^{4/3} T^2\rho_q^{1/3} + \cdots\right]$$

$$\mu_q = T\eta_q(\rho_q, T) + \left(\frac{\partial E}{\partial \rho_q}\right) - \vec{\nabla}\cdot\left(\frac{\partial E}{\partial \vec{\nabla}\rho_q}\right)$$

$$P = \sum_q \frac{2}{3}E_{Kq}^* + \sum_q\left[\left(\frac{\partial E}{\partial \rho_q}\right)\rho_q - \vec{\nabla}\cdot\left(\frac{\partial E}{\partial \vec{\nabla}\rho_q}\right)\rho_q\right] - U$$

At high T or low density, small $\rho\lambda^3$ (nearly nondegenerated Fermi gas)

$$\eta_q = \beta \frac{p_{Fq}^2}{2m_q^*} = \ln\left[\left(\frac{\rho_q\lambda_q^3}{\gamma}\right)\left(1+\frac{1}{2\sqrt{2}}\frac{\rho_q\lambda_q^3}{\gamma}+\cdots\right)\right] \approx \ln\left(\frac{\rho_q\lambda_q^3}{\gamma}\right)+\frac{1}{2\sqrt{2}}\frac{\rho_q\lambda_q^3}{\gamma}+\cdots$$

$$E_{Kq}^* = \frac{\hbar^2}{2m_q^*}\tau_q = \frac{3}{2}\rho_q T\left[1+\frac{1}{2^{5/2}}\left(\frac{\rho_q\lambda_q^3}{\gamma}\right)+\left(\frac{1}{8}-\frac{2}{3^{5/2}}\right)\left(\frac{\rho_q\lambda_q^3}{\gamma}\right)^2+\cdots\right]$$

$$TS = \frac{5}{2}T\rho - T\sum_q \rho_q \ln\left(\frac{\rho_q\lambda_q^3}{\gamma}\right)+\frac{T}{2\sqrt{2}}\sum_q\left(\frac{\rho_q\lambda_q^3}{\gamma}\right)\left(\frac{\rho_q}{4}\right)$$

$$\lambda_q = \sqrt{2\pi\hbar^2/m_q^*T}$$

$$\mu_q = T\ln\left[\left(\frac{\lambda_q^3}{\gamma}\right)\rho_q\right] + \frac{T}{2\sqrt{2}}\left(\frac{\lambda_q^3}{\gamma}\right)\rho_q$$

$$+\frac{1}{4}\left[t_1\left(1+\frac{x_1}{2}\right)+t_2\left(1+\frac{x_2}{2}\right)\right]\frac{3}{2}T\sum_q\frac{2m_q^*}{\hbar^2}\left[\rho_q+\frac{1}{2^{5/2}}\left(\frac{\lambda_q^3}{\gamma}\right)\rho_q^2\right]$$

$$-\frac{1}{4}\left[t_1\left(\frac{1}{2}+x_1\right)-t_2\left(\frac{1}{2}+x_2\right)\right]\frac{3}{2}T\frac{2m_q^*}{\hbar^2}\left[\rho_q+\frac{1}{2^{5/2}}\left(\frac{\lambda_q^3}{\gamma}\right)\rho_q^2\right]$$

$$+t_0\left(1+\frac{x_0}{2}\right)\rho+\frac{t_3}{12}\left(1+\frac{x_3}{2}\right)(\alpha+2)\rho^{\alpha+1}-t_0\left(\frac{1}{2}+x_0\right)\rho_q$$

$$-\frac{t_3}{12}\left(\frac{1}{2}+x_3\right)\alpha\rho^{\alpha+1}+\frac{t_3}{12}\left(\frac{1}{2}+x_3\right)(\alpha-1)2\rho^{\alpha}\rho_q-\frac{t_3}{12}\left(\frac{1}{2}+x_3\right)2\alpha\rho^{\alpha-1}\rho_q^2$$

$$+C\beta\rho^{\beta-1}\rho_p^2+2C\rho^{\beta}\rho_p\delta_{q,p}+\eta C_S\rho^{\eta-1}$$

$$P=\frac{5}{2}T\rho+\frac{5}{2}\frac{T}{2\sqrt{2}}\sum_q\left(\frac{\lambda_q^3}{\gamma}\right)\left(\frac{\rho_q^2}{2}\right)-\frac{3}{2}T\sum_q\frac{m_q^*}{m}\left[\rho_q+\frac{1}{2\sqrt{2}}\left(\frac{\lambda_q^3}{\gamma}\right)\left(\frac{\rho_q^2}{2}\right)\right]$$

$$+\frac{t_0}{2}\left(1+\frac{x_0}{2}\right)\rho^2+\frac{t_3}{12}\left(1+\frac{x_3}{2}\right)(\alpha+1)\rho^{\alpha+2}-\frac{t_0}{2}\left(\frac{1}{2}+x_0\right)\sum_q\rho_q^2-\frac{t_3}{2}\left(\frac{1}{2}+x_3\right)\rho^{\alpha}\sum_q\rho_q^2$$

$$+C(\beta+1)\rho^{\beta}\rho_p^2+C_S(\eta-1)\rho^{\eta}$$

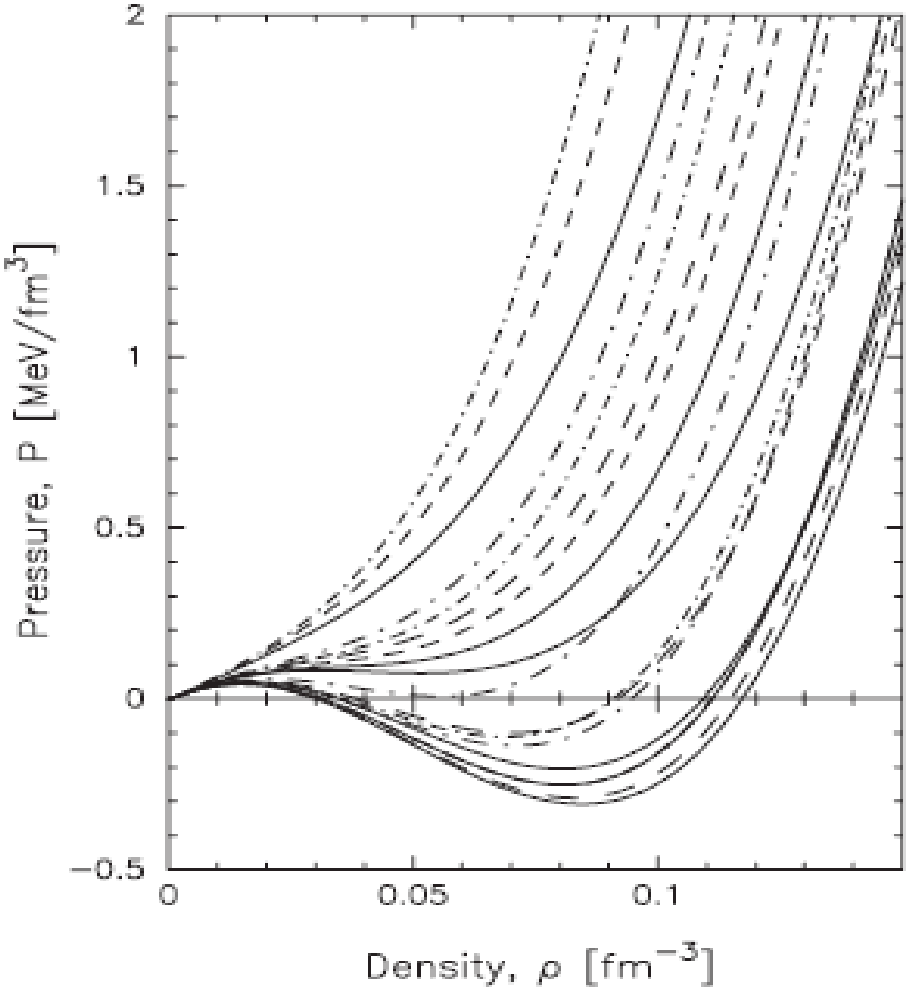

FIG. 1. Equation of state $P(\rho)$ for fixed $y = 0, 0.2, y_m(\rho)$ [the proton concentration with minimum pressure defined by Eq. (10)] for thick lines from top to bottom and $y = 0.5, 0.8, 1.0$ for thin lines from bottom to top. The solid line is for the modified SKM($m^* = m$) interaction with both isoscalar and isovector momentum-dependent terms, the dash-dotted line is for a momentum-dependent but isovector-independent term, and the dashed line is for momentum-independent terms only. The lowest thin dashed curve overlaps here with the lowest thin solid curve that have $y = 0.5$.

S.J. Lee
A.Z. Mekjian
PRC79,044323(2009)

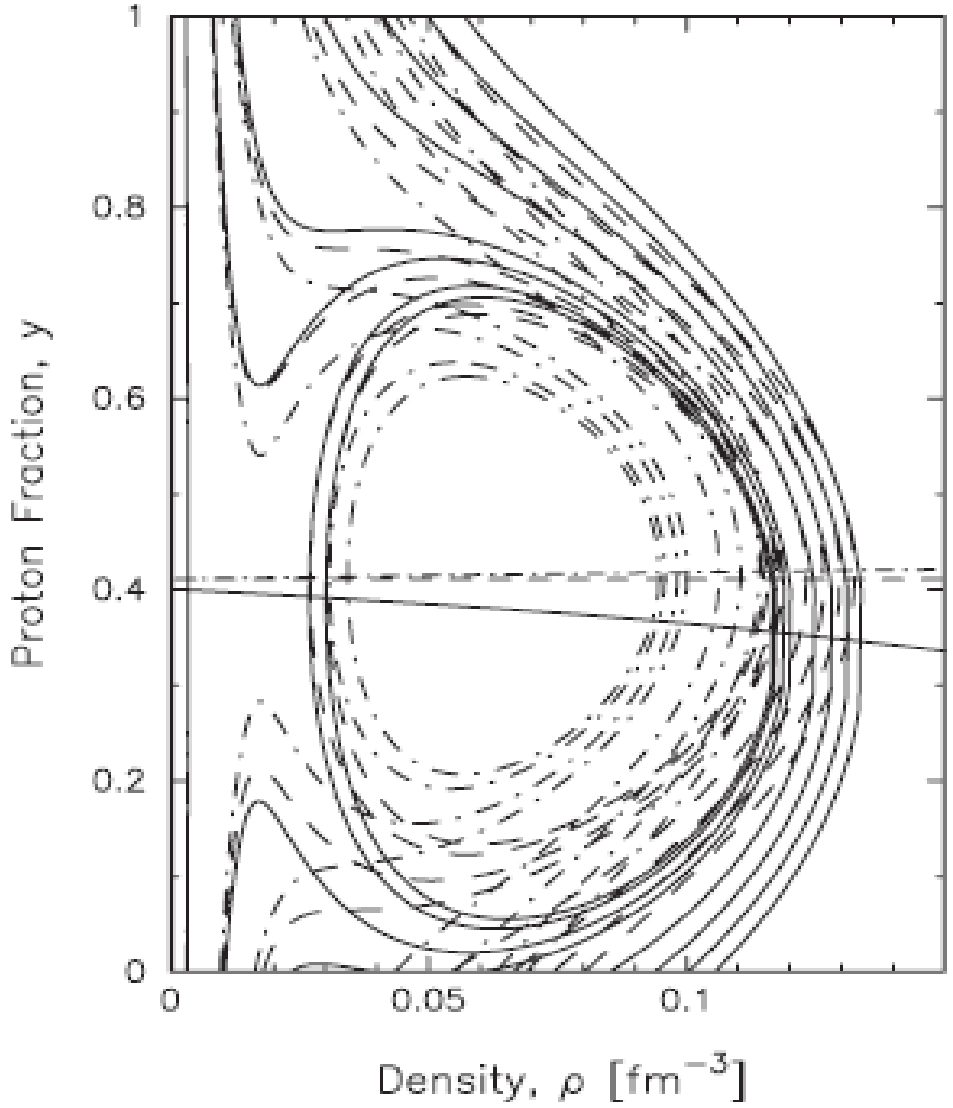

FIG. 2. The $y(\rho)$ dependence for fixed pressure of $P = 0, 0.015,$ 0.05, 0.08, 0.2, 0.3, 0.4, 0.5 MeV fm^{-3}. The curves are the same as those described in the caption to Fig. 1. The thin horizontal lines are for $y_m(\rho)$ curve define by Eq. (10).

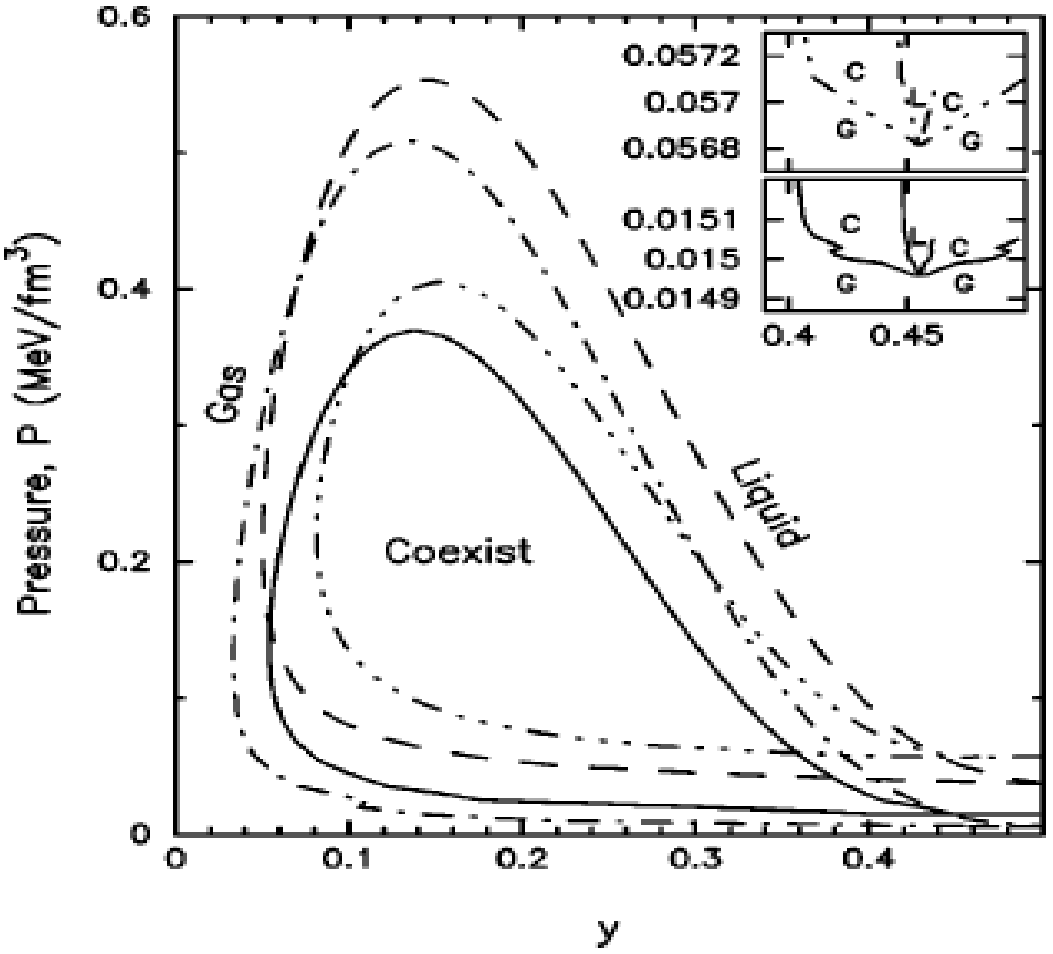

S.J. Lee
A.Z. Mekjian
PRC63,044605(2001)

FIG. 4. Binodal curve at $T = 10$ MeV. The solid curve is for the case with Coulomb and surface effects, the dash-dotted curve is for the case with surface effects, the dash-dot-dot-dotted curve is for the case with Coulomb interactions, and the dashed curve is for the case without Coulomb and surface effects. Small boxes at the upper right corner are the expansion of the main figure. In the small boxes, the region of liquid, gas, and coexistence are indicated by L, G, and C, respectively.

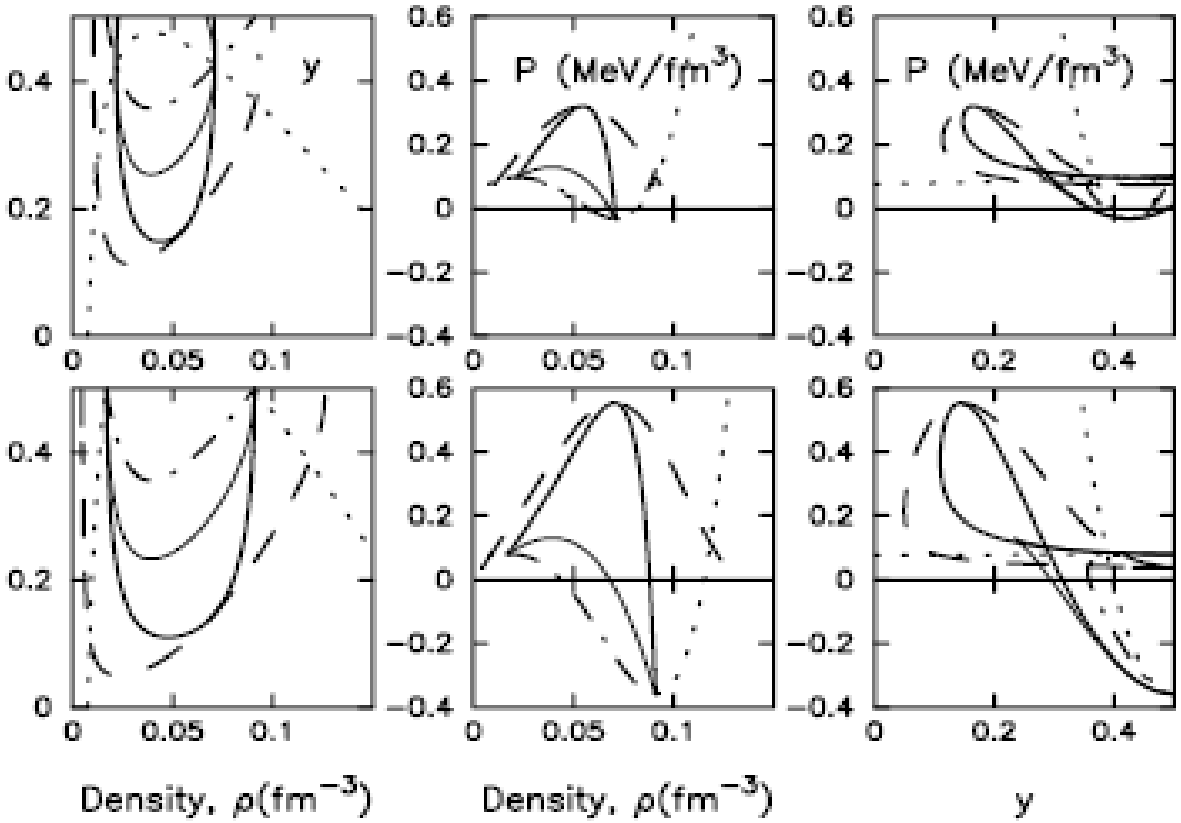

FIG. 1. Chemical (thick solid curve) and mechanical (thin solid curve) instability curves at temperature $T=10$ MeV with (upper boxes) and without (lower boxes) Coulomb effects arising from a $R=8$ fm uniform sphere. The dashed curves are the coexistence curve at $T=10$ MeV. The dotted curves are for $(d\mu_p/d\rho)_{y,T}=0$ and the dash-dotted curves are for $(d\mu_n/d\rho)_{y,T}=0$. The equal concentration $y_E=0.4256$ at $T=10$ MeV. The curves are the constant T plane cuts of the corresponding surfaces in (ρ,y,T) space (left column), in (ρ,P,T) space (center column), and in (P,y,T) space (right column).

S.J. Lee
A.Z. Mekjian
PRC68,14608(2003)

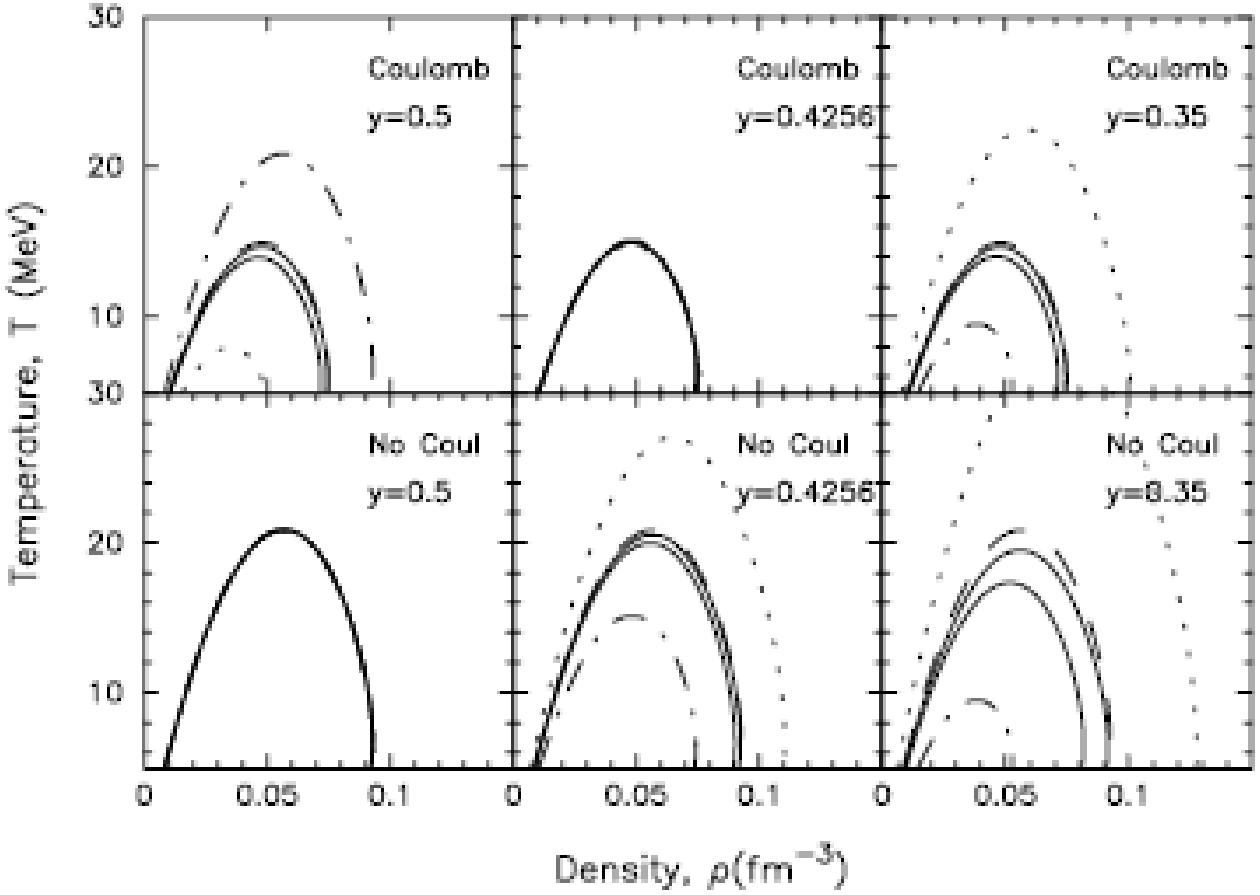

FIG. 2. The temperature dependence of the chemical and mechanical instability curves at a fixed proton concentration y. The curves here are the constant y plane cuts of the corresponding surfaces in (ρ, y, T) space. The curves are the same as in Fig. 1 except the dashed curves. With the temperature dependent equal concentration $y_E(T)$, all the curves coincide as shown by a dashed line here [note here that $y_E(T) = 1/2$ without Coulomb force].

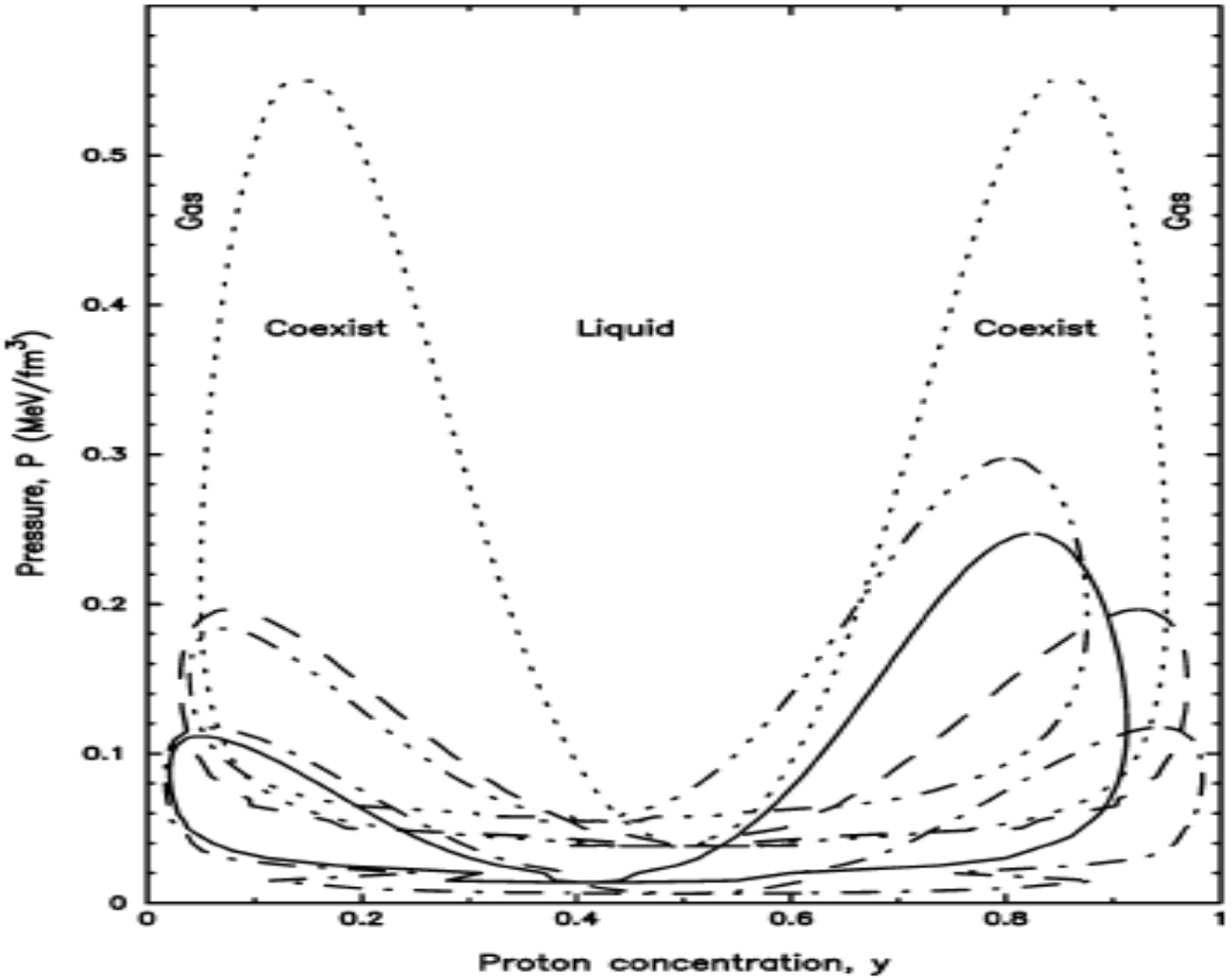

Fig. 1. Pressure P versus proton fraction y for coexistence loop at $T = 10$ MeV. The solid line is for the case with Coulomb and surface effects. The dash-dotted line has surface, but no Coulomb terms. Coulomb effects are shown in the dash-dot-dot-dotted line with no surface terms. The dashed line is for the case without Coulomb and surface terms while the dotted line is for a larger symmetry energy. The regions of liquid and gas phases and the coexistence are indicated explicitly for the dotted curve. (We believe that some zig zag behavior appearing on curves at small pressure comes from a numerical error even though we were not able to remove it.)

S.J. Lee
A.Z. Mekjian
PLB580,137(2004)

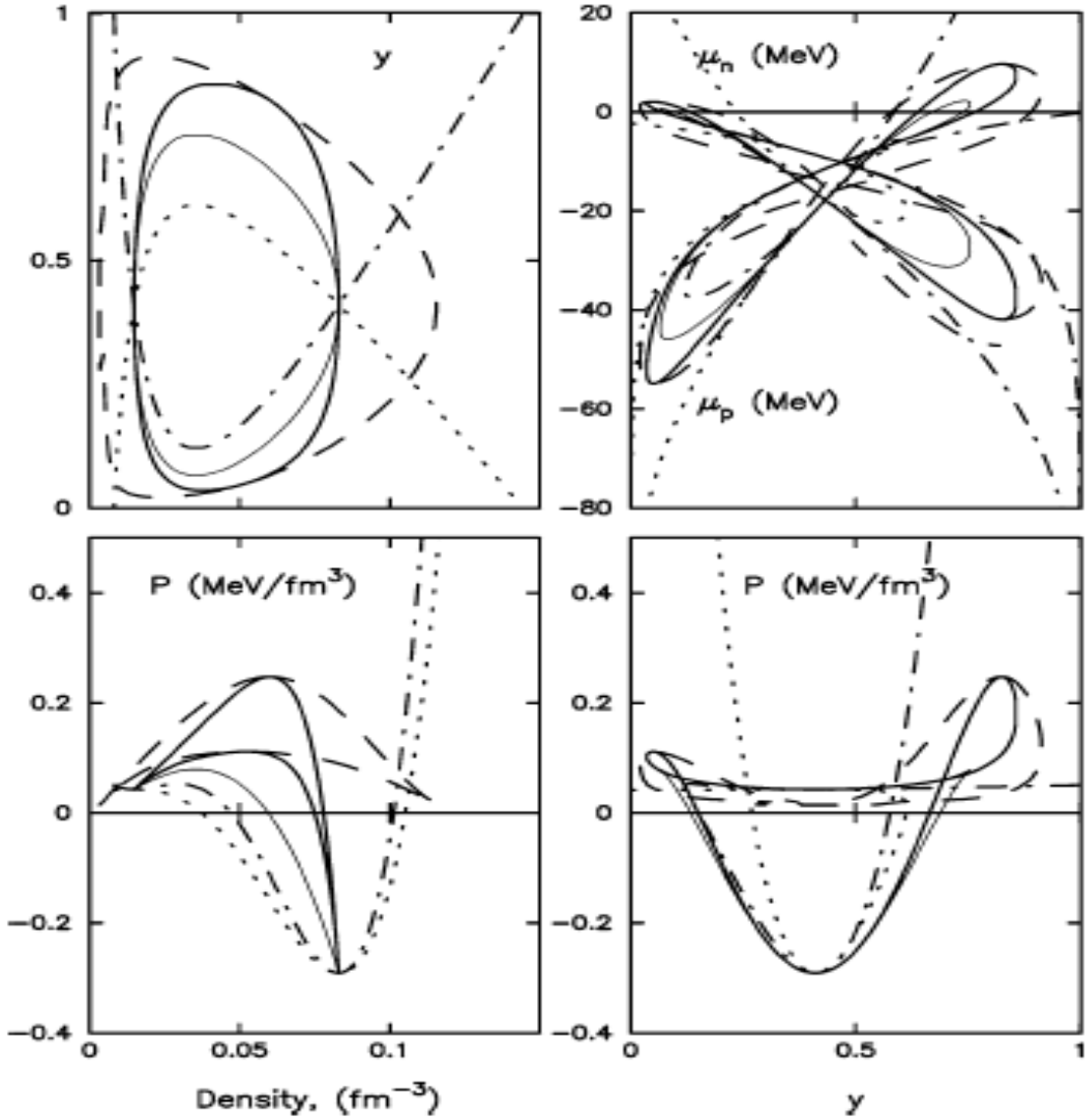

Fig. 2. Figures show the coexistence curves (dashed line), chemical instability curves (thick solid line) and mechanical instability curves (thin solid line). Also shown are the $\partial\mu_q/\partial\rho = 0$ curves for proton (dotted line) and for neutron (dash-dotted line) at $T = 10$ MeV. The Coulomb and surface terms are included here.

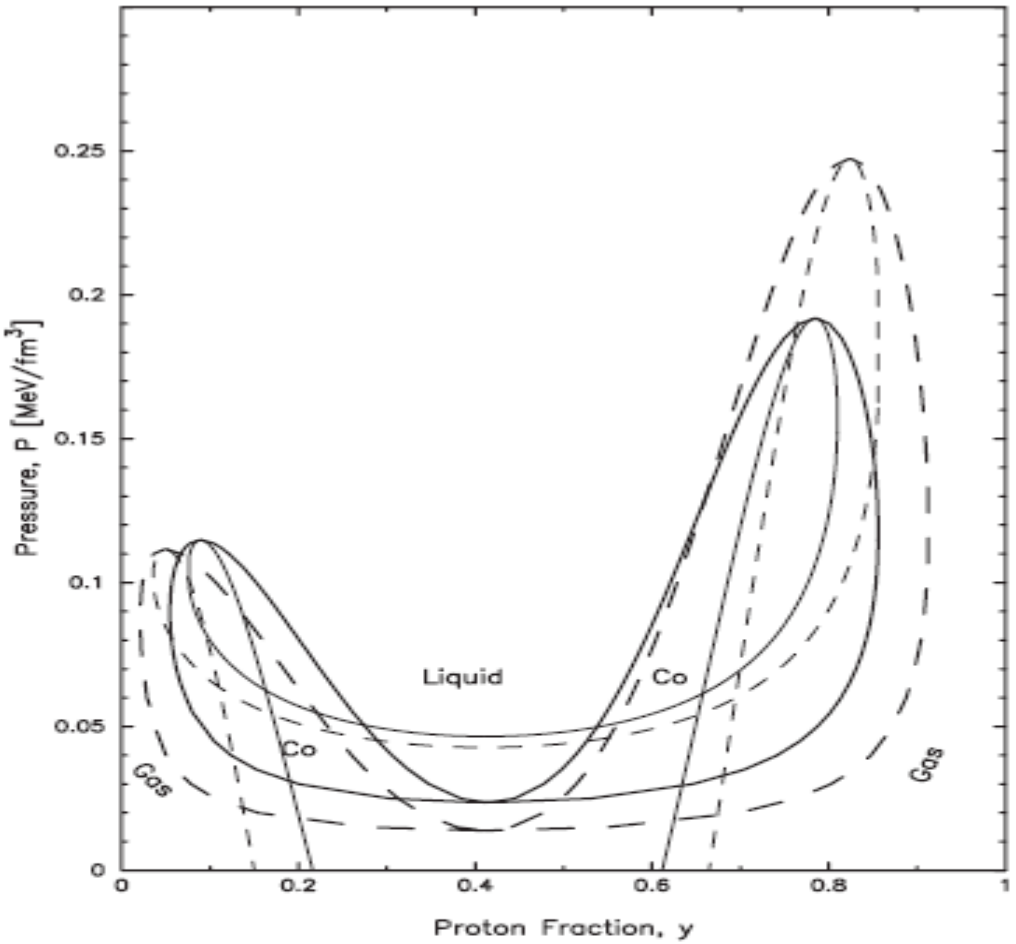

FIG. 5. Pressure P vs proton fraction y for coexistence loop (thick curves) at $T = 10$ MeV. The solid curve is for the momentum-dependent Skyrme force and the dashed curve is for the momentum-independent Skyrme force. The thin curves are the chemical instability boundary curves for each case of Skyrme interaction respectively. For both momentum-dependent and momentum-independent cases the maxima of the chemical instability loop and the coexistence loop occur at the same point where the curves are tangent to each other as discussed in the text. The point of equal concentration is $y_E \sim 0.415$ for the momentum-dependent case and $y_E = 0.41057$ for the momentum-independent case.

S.J. Lee
A.Z. Mekjian
PRC77,054612(2008)

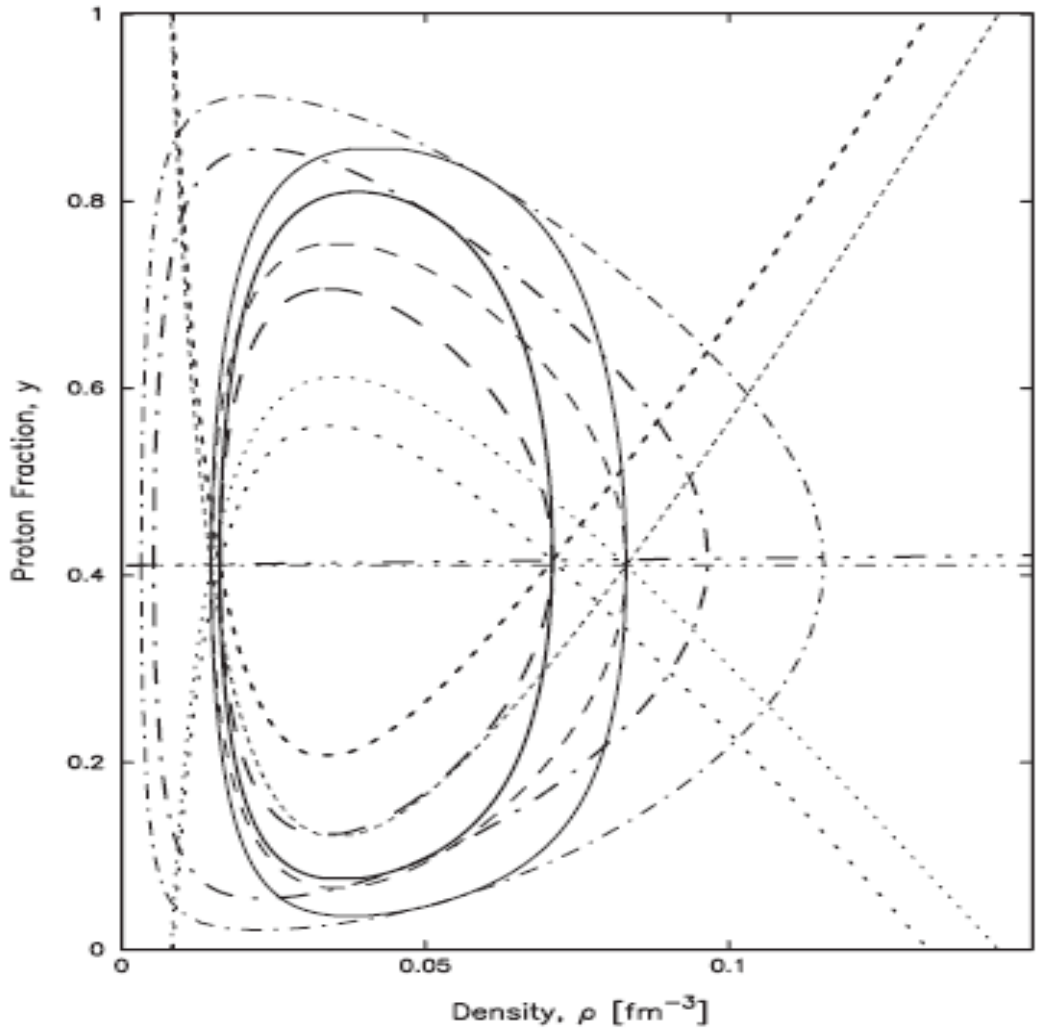

FIG. 6. The coexistence curves (dash-dotted line), chemical instability boundary curves (solid line), and mechanical instability boundary curves (dashed line) at $T = 10$ MeV. Also shown are the $\partial\mu_q/\partial\rho = 0$ curves for protons (dotted line) and for neutrons (short dash line) at $T = 10$ MeV. The dash-triple-dotted line is for $y_E(\rho)$. The thick lines are for the momentum-dependent Skyrme force and the thin lines are for the momentum-independent Skyrme force. The momentum-dependent loops are inside the momentum-independent loops.

Thick: inside
Thin; outside

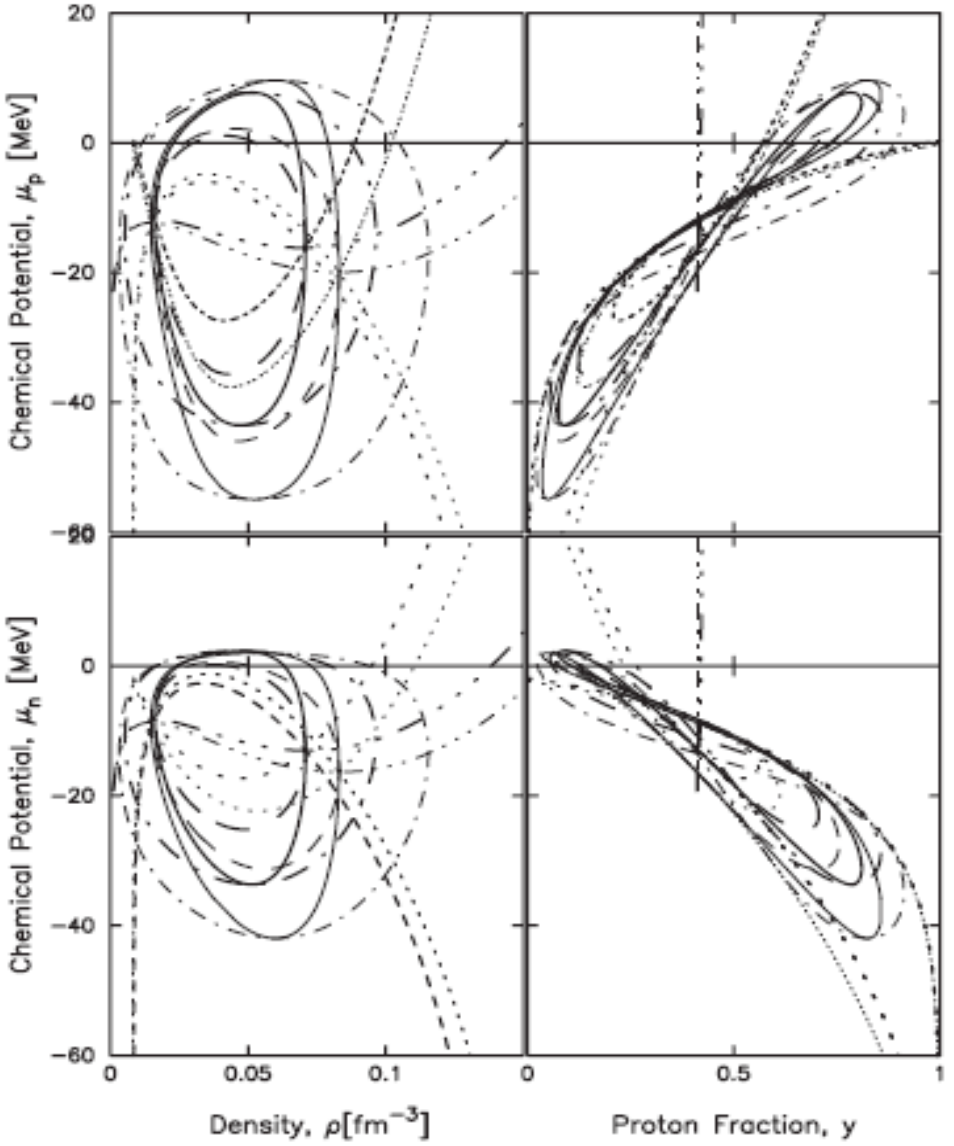

FIG. 7. Chemical potential μ_p (upper panel) and μ_n (lower panel) for various boundary curves at $T = 10$ MeV. The meanings of the curves are the same as in Fig. 6.

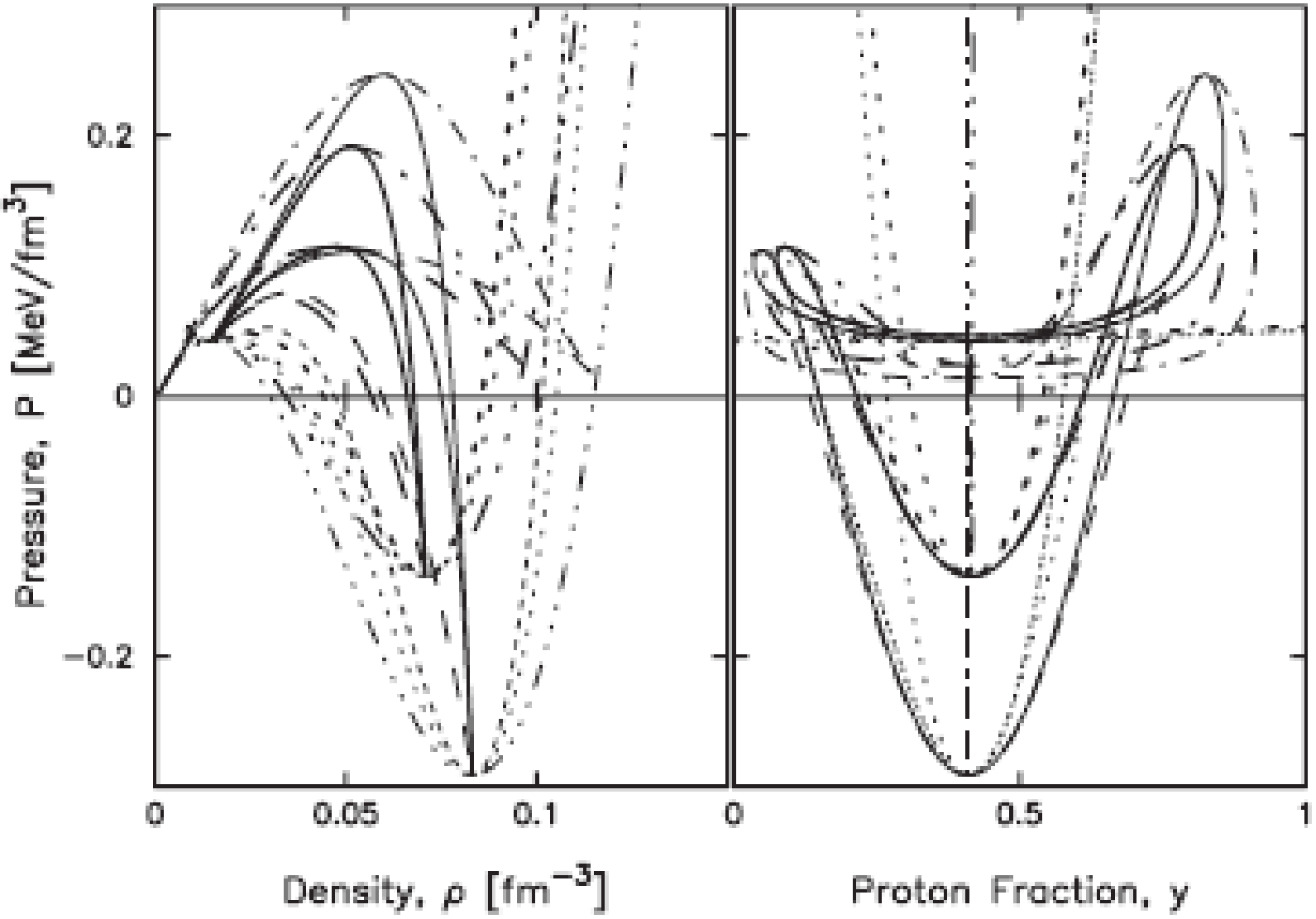

FIG. 8. Pressure P for various curves. The meanings of the curves are the same as in Fig. 6.

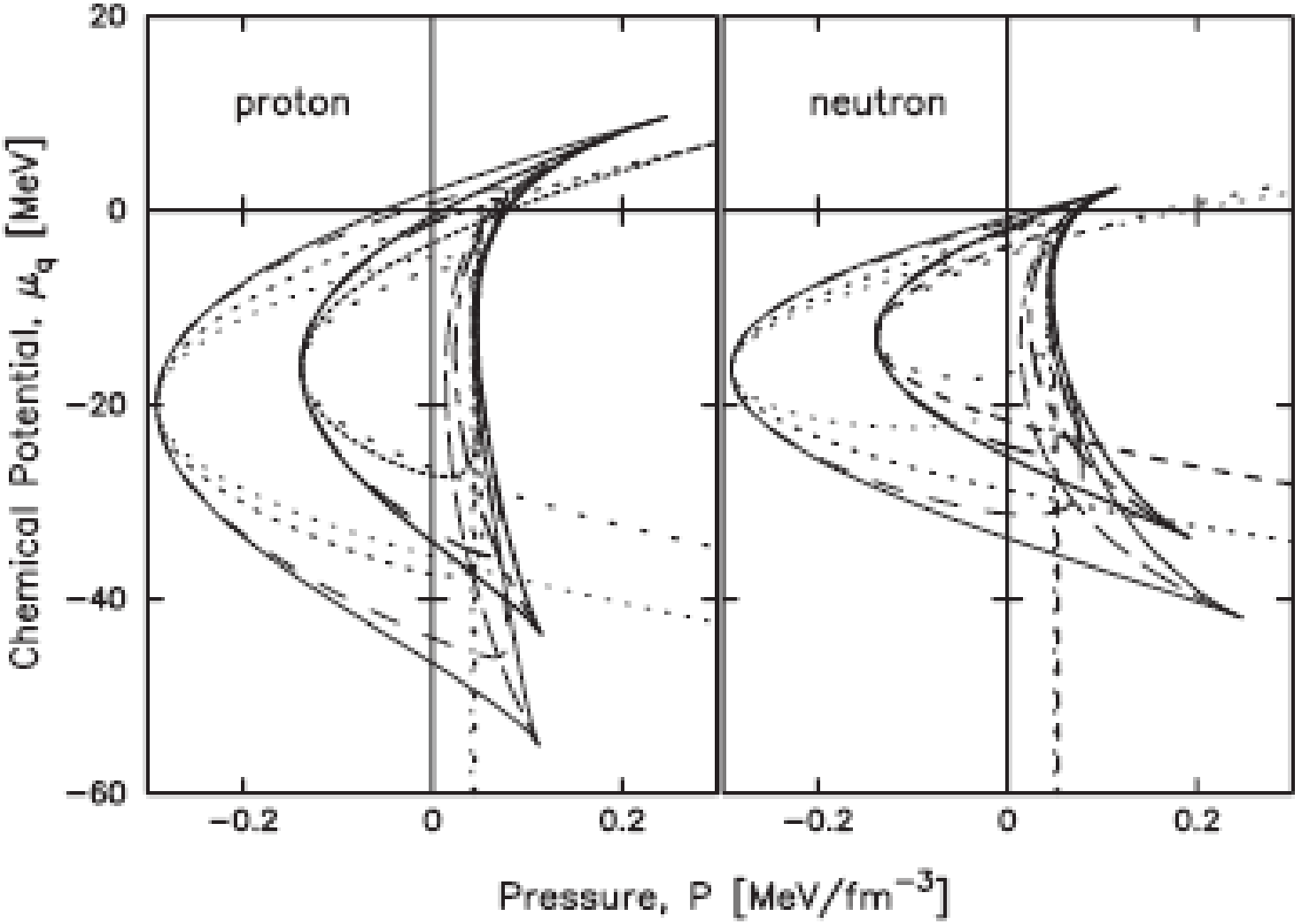

FIG. 9. Chemical pressure μ_q vs pressure P for various boundary curves. The left panel is for the proton μ_p and the right panel is for the neutron μ_n. The meanings of the curves are the same as in Fig. 6.

TABLE I. Skyrme parameters are in MeV and fm units. First three columns are from the SKM($m^* = m$) parameter set [1,27] except $x_0 = -1/6$ and $x_3 = -1/2$. The last column is from the SLy4 parameter set [28]. The nuclear matter properties at the saturation are also shown. The effective mass is for a saturated symmetric nuclear matter.

	SKM($m^* = m$)			SLy4
		No isovector	Momentum indep.	
t_0	−1089.0	−1089.0	−1089.0	−2488.91
x_0	−1/6	−1/6	−1/6	0.834
t_3	17270	17270	17270	13777.0
x_3	−1/2	−1/2	−1/2	1.354
α	1	1	1	1/6
t_1	251.11	251.11	0	486.82
x_1	0	−1/2	0	−0.344
t_2	−150.66	−150.66	0	−546.39
x_2	0	−1/2	0	−1.000
Effective mass m^*/m	0.999987	0.894430	1	0.694658
Binding energy E_B/A	15.8173	13.3250	15.8176	15.9722
Fermi energy E_F	34.5186	32.0728	34.5188	36.7743
Saturation density ρ_0	0.14509	0.12994	0.14509	0.15954
Symmetry energy S_V	18.6080	23.7451	24.6730	32.0038
Compresibility κ	367.556	312.281	367.562	229.901

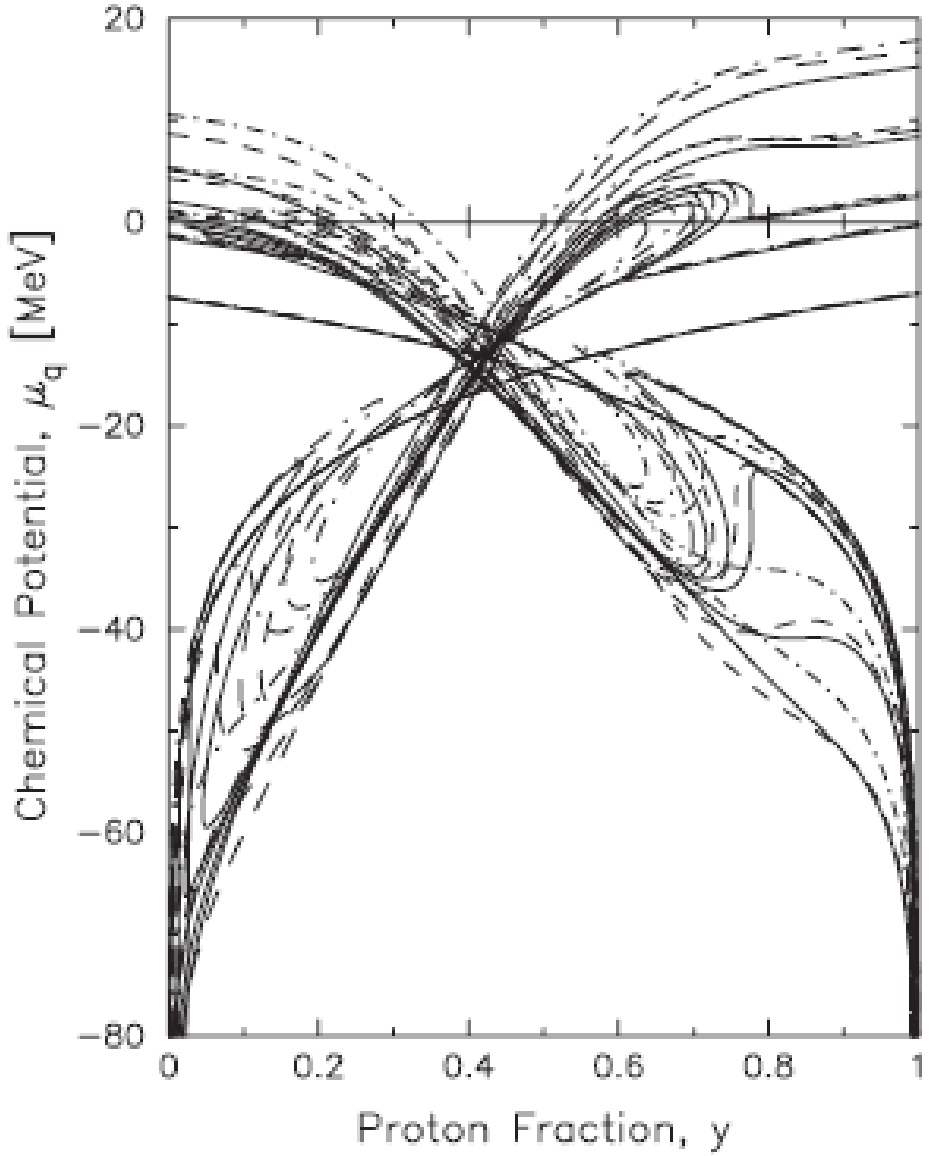

FIG. 3. Chemical potential μ_p (thick lines) and μ_n (thin lines) as a function of y for $P = 0.015$, 0.05, 0.08, 0.2, and 0.5. The curves are the same as in Fig. 1.

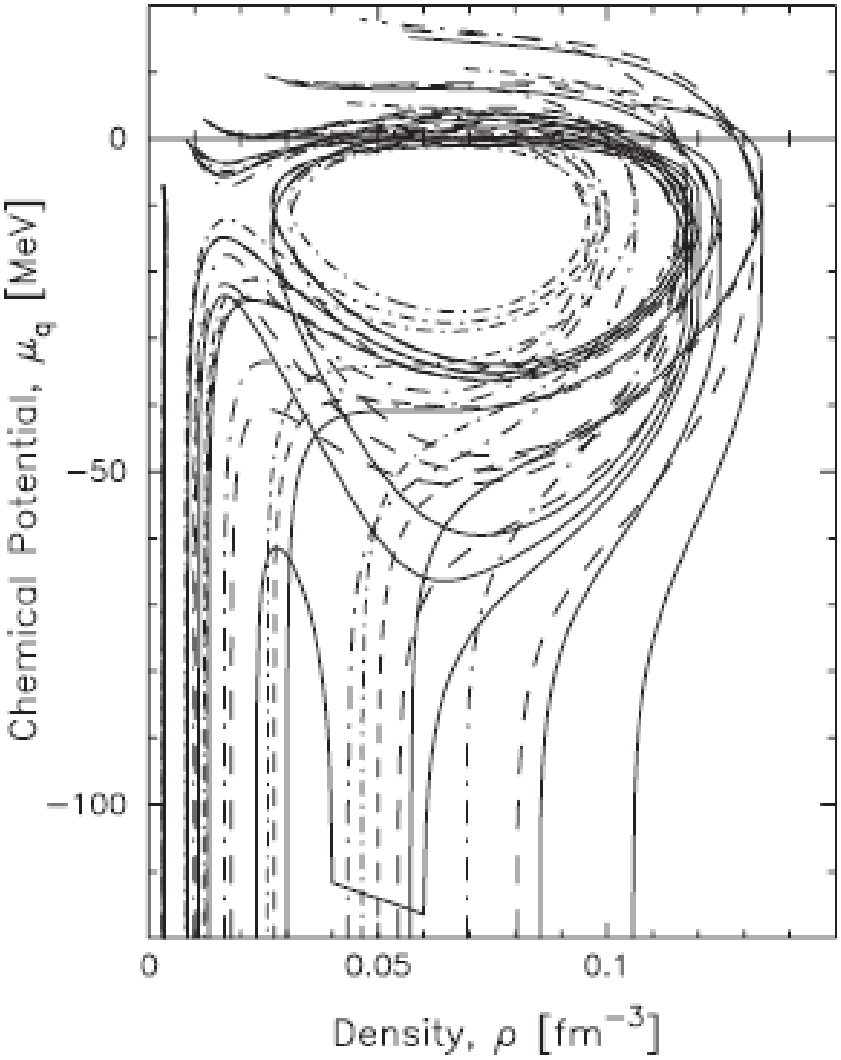

FIG. 4. Same as Fig. 3 but as a function of ρ. The straight horizontal portion of the thick solid curve (momentum-dependent force with both isoscalar and isovector terms) for $P = 0.08$ MeV/fm^3 at low μ_p just represents the cut in the density range of $0.04 < \rho < 0.06$ fm^{-3} due to the condition of $y \geqslant 0$.

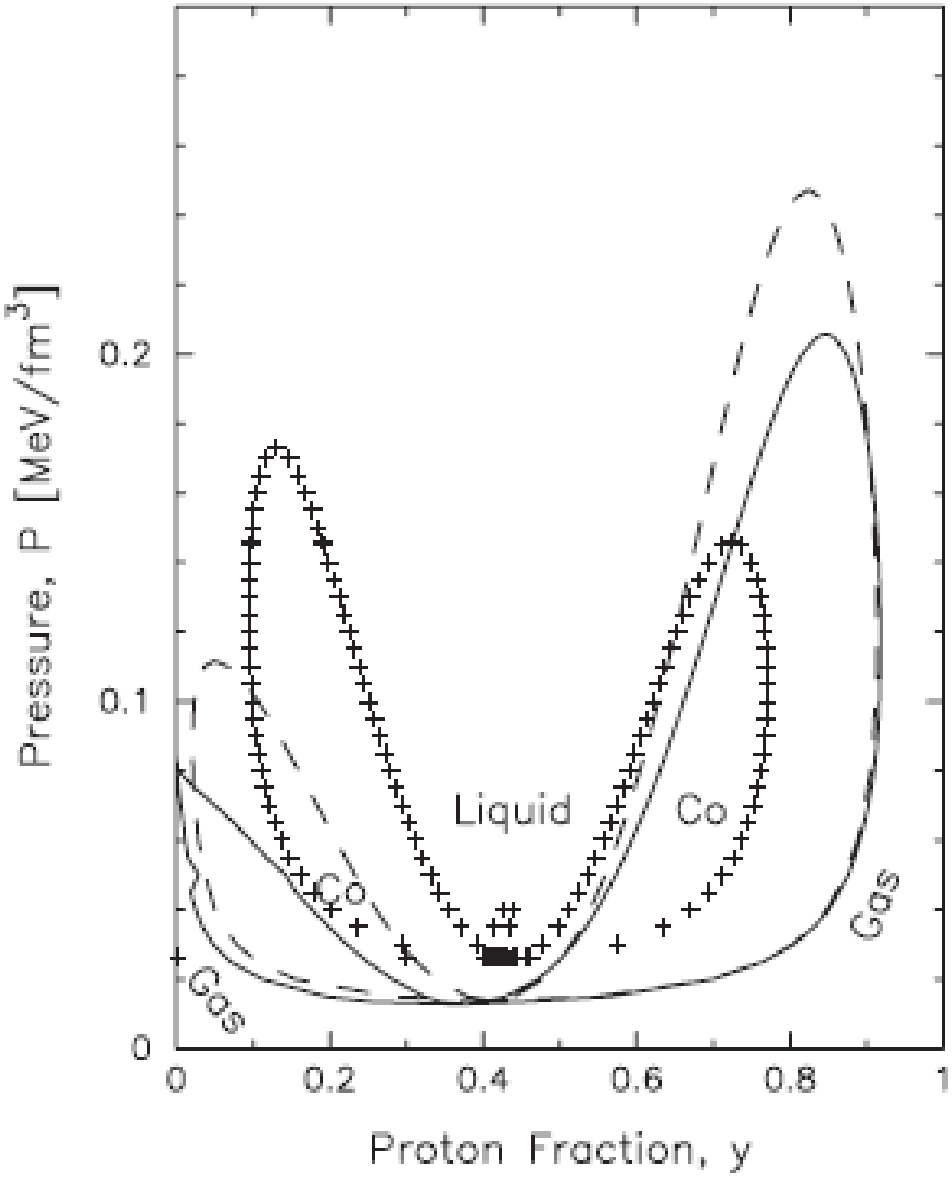

FIG. 5. $P(y)$ plot for coexistence curve. The curves are the same as in Fig. 1 . The curve with + sign is for SLy4 parameter.

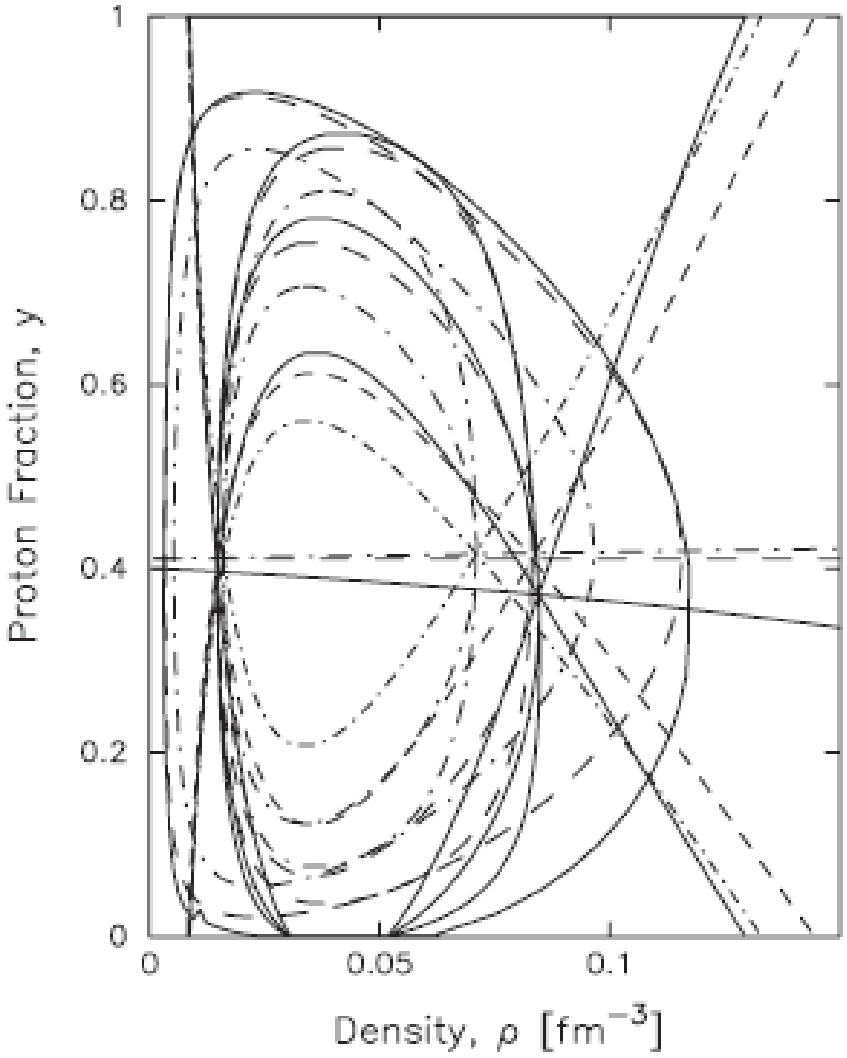

FIG. 6. The closed loops are for coexistence curves, chemical instability boundary curves, and mechanical instability curves from outmost loops to inside loops at $T = 10$ MeV. Also shown by thin lines are $\partial\mu_q/\partial\rho = 0$ for proton (opened downward) and for neutron (opened upward). The horizontal lines are the $y_m(\rho)$ determine by Eq. (10).

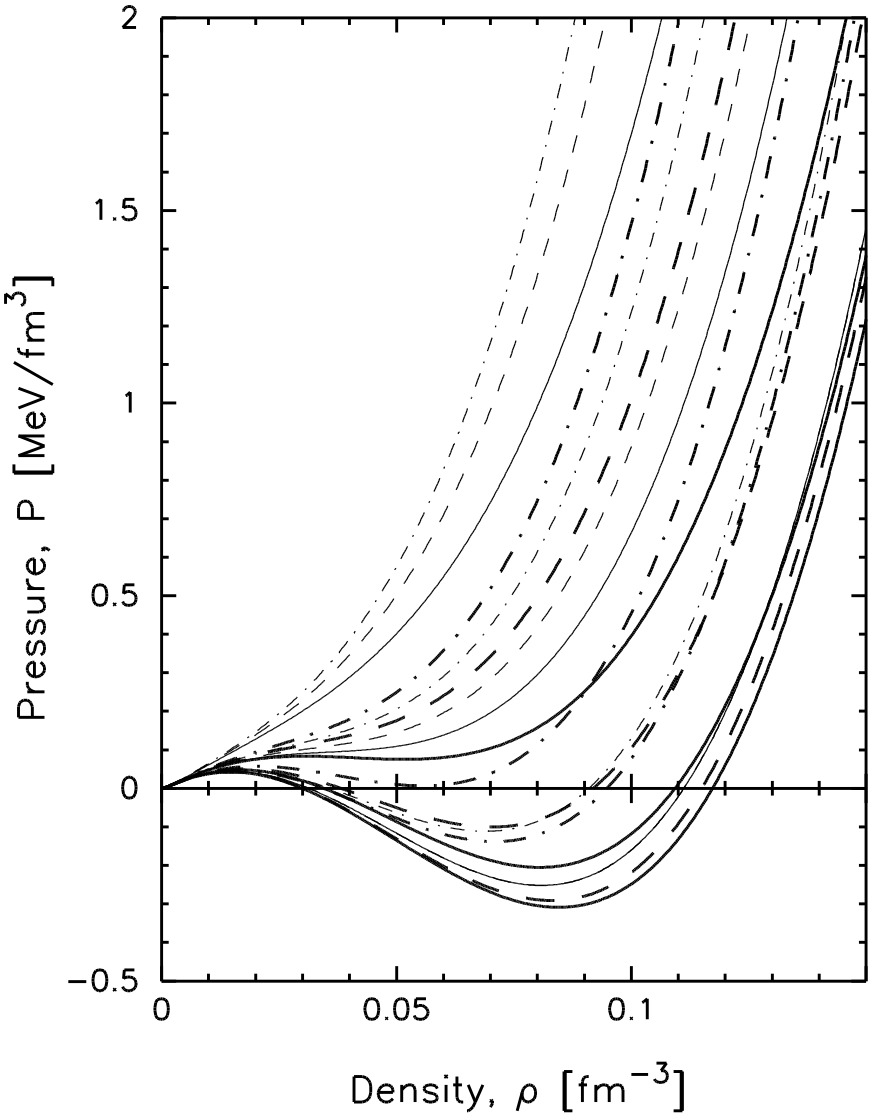
Pressure, P [MeV/fm^3]
Density, ρ [fm^{-3}]
2
1.5
1
0.5
0
−0.5
0
0.05
0.1

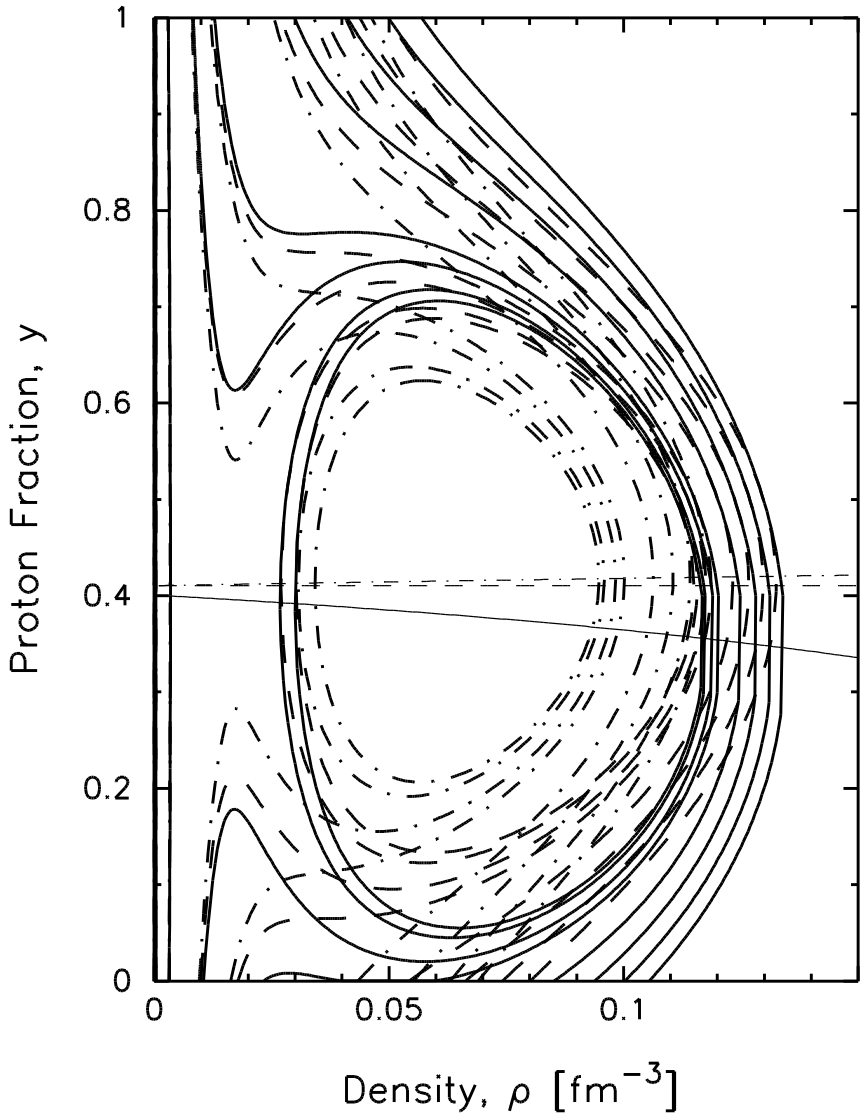
Proton Fraction, y
Density, ρ [fm^{-3}]
1
0.8
0.6
0.4
0.2
0
0
0.05
0.1

Summary

- Surface tension: lower pressure of coexistence binodal surface (toward P=0)
- Coulomb interaction: Shrink binodal region and mechanical and chemical instability region, move LEC to lower y_E than 0.5, cross of μ_p curves in y for different P, asymmetric pair of LG at higher $y > y_E$, two pairs meet together with lowest P at y_E
- Symmetry energy: $y_G > y_L$ for $y > y_E$ and $y_G < y_L$ for $y < y_E$, larger symmetry energy make higher pressure and narrower coexistence loop, loops are closer to y_E, tend to restore symmetry of loops
- Value of y_E for LEC is somewhat insensitive to nuclear force, value of pressure is more sensitive

- Mechanical instability loop is inside of chemical instability boundary and tangent at y_E – diffusive chemical transition occurs even in mechanically stable region
- Chemical instability loop is inside of coexistence loop and tangent to it at their maxima in P
- At y_E , all curves coincide in ρ–T plot, phase transition behaves same as one component system
- For $y < y_E$, neutron diffusion is important, while proton diffusion for $y > y_E$
- Momentum dependent isoscalar makes pressure higher while isovector momentum dependent term makes much lower for given density and y
- Momentum dependent isoscalar makes loops smaller while momentum dependent isovector term makes loops more larger

- Momentum dependent isoscalar makes coexistence loop closer to y_E while momentum dependent isovector term makes loop away
- Momentum dependent term lower the height of coexistence loop at proton rich side while it remains similar at neutron rich side
- Momentum dependent isovector term has opposite and larger effect than isoscalar momentum dependent term
- Isovector term make symmetry energy smaller and thus loops become more asymmetric
- For SLy4 left coexistence loop of lower proton fraction is more pronounced than right loop of high proton fraction, isoscalar and isovector have same sign
- SLy4 loop at higher y is narrower in y than loop for SKM(m*=m)
- Symmetry energy has important role in coexistence

- Surface tension; lower pressure of coexistence binodal surface (to P=0)
- Coulomb interaction; shrink binodal loop, cross of chemical potential curves in y for different P at near y=0.5, move LEC to smaller yE than 0.5 for symmetric system, asymmetric pair of L-G at higher y > yE, two pairs meet together with lowest P at yE
- Value of yE is somewhat insensitive to nuclear force, pressure is more sensitive
- Symmetry energy; Larger y in gas and smaller y in liquid for y > yE, opposite for y < yE
- Nonlinear density dependence of symmetry energy
- Coulomb shrink chemical & mechanical instability region
- Mechanical is inside of chemical and tangent at yE, diffusive chemical transition occurs even in mechanically stable region, same at yE
- Chemical is inside of coexitence and tangent to it at maxima
- At yE, peak in chemical instability and binodal surface coincide,
- For y.ne.yE In T vs rho, paks for chemical instability and coexistence coincide, but peak of mrchanical or spinodal instability is below of others
- At y = yE, phase transition behaves same as one component system keeping y=yE in both phase
- For y < yE, neutron diffusion is important, while proton diffusion for y < yE
- Momentum dependence increase pressure at given density
- Momentum dependence make smaller boundaries
- Reduce height of coexistence loop at proton rich side and remain similar at neutron rich side, increase lowest pressure of coexistence curve
- Largest and smallest y in coexitence loops shifted toward yE

- For SLy4 left coexistence loop of lower proton fraction is more pronounced than right loop of high proton fraction, isoscalar and isovector have same sighn
- For SKM(m*=m) right loop is more pronounced than left loop, isoscalar term raises pressure of loop on neutron rich side while isovector lowers due to opposite sighn of force
- SLy4 loop at higher y is narrower in y than loop for SKM(m*=m), SLy4 has higher symmetry energy
- Higher left loop means liquid and gas can coexist at higher pressurewith more neutron rich gas and lesser rich neutron liquid for left loop
- Narroing of coexistence loop brings yG and yL closer together thereby reducing proton fraction differece in gas and liquid phase
- Momentum dependent isovector term has opposite and larger effect than isoscalar momentum dependent term
- Isovector tem make symmetry energy smaller and thus loops become more adsymmetric
- Pressure for given rho, y, T becomes larger by isoscalar term while it becomes smaller by isovectoer term
- Symmetry energy terms tend to restore dymmetry of loops
- Loops for SKM(m*=m) with both isoscalar and isovector terms have smallest symmetry energy, has cut at y=0
- Loops for SLy4 with largestsymmetry energy, are closer to its yE than SKM(m*=m)

For Skyme Hamiltonian of

$$H(\rho_q, \nabla\rho_q, \tau_q) = E^*_{Kp} + E^*_{Kn} + U(\rho_q, \nabla\rho_q)$$

$$E^*_{Kq}(\rho_q, \tau_q) = \frac{\hbar^2}{2m^*_q}\tau_q = \frac{\hbar^2}{2m_q}\tau_q + \frac{\hbar^2}{2m_q}(a\rho + b\rho_q)\tau_q$$

$$U(\rho_q, \nabla\rho_q) =$$ Momentum Independent Interaction

$$\rho_q = \int d^3p \quad f_q(\vec{r}, \vec{p})$$

$$\tau_q = \int d^3p \quad \frac{p^2}{\hbar^2} \quad f_q(\vec{r}, \vec{p}), \qquad \vec{j}_q = \int d^3p \quad \frac{\vec{p}}{\hbar} \quad f_q(\vec{r}, \vec{p})$$

$$f_q(\vec{r}, \vec{p}) = \frac{\gamma}{h^2}\tilde{f}_q(\vec{r}_q, \vec{p}) = \frac{\gamma}{h^2} \quad \frac{1}{1 + e^{\beta[\varepsilon_q(\vec{r}, \vec{p}) - \mu_q]}} = \frac{\gamma}{h^2} \quad \frac{1}{1 + e^{\beta\frac{p^2}{2m^*_q} - \eta_q}}$$

For Consistency

$$T\eta_q(\rho_q,T)=\left(\frac{\partial E}{\partial \tau_q}\right)\frac{p_{Fq}^2}{\hbar^2}=\sum_{q'}\left(\frac{\partial E}{\partial \tau_{q'}}\right)\left(\frac{\delta \tau_{q'}}{\delta \rho_q}\right)-T\left(\frac{\delta S}{\delta \rho_q}\right)$$

$$\sum_{q'}\left[\left(\frac{\partial E}{\partial \tau_{q'}}\right)\left(\frac{\delta \tau_{q'}}{\delta \rho_q}\right)-\frac{5}{3}\left(\frac{\delta E^*_{Kq'}}{\delta \rho_q}\right)+T\left(\frac{\delta \eta_{q'}}{\delta \rho_q}\rho_{q'}\right)\right]=0$$